Chromosome-scale genome assembly of the European common cuttlefish *Sepia officinalis*

Simone Rencken[1,2] https://orcid.org/0009-0003-9341-2898, Georgi Tushev[1] https://orcid.org/0000-0002-3340-9422, David Hain[1,3] https://orcid.org/0000-0002-8979-7938, Elena Ciirdaeva[1] https://orcid.org/0009-0000-7360-7725, Oleg Simakov[4] https://orcid.org/0000-0002-3585-4511, Gilles Laurent[1] https://orcid.org/0000-0002-2296-114X

[1] Max Planck Institute for Brain Research, Frankfurt am Main, Germany
[2] Radboud University, Donders Institute for Brain, Cognition and Behaviour, Nijmegen, Netherlands
[3] Faculty of Biological Sciences, Goethe University, Frankfurt am Main, Germany
[4] Department of Neuroscience and Developmental Biology, University of Vienna, Vienna, Austria

Abstract

Coleoid cephalopods, a subclass of mollusks, exhibit remarkable adaptations, including the largest brains among invertebrates, camera-like eyes, and a distinctive embryonic development. They possess an advanced behavioral repertoire including dynamic camouflage.

The common cuttlefish *Sepia officinalis* has served as a key model organism in various research fields, spanning biophysics, neurobiology, behavior, evolution, ecology and biomechanics. More recently, it has become a model to investigate the neural mechanisms underlying cephalopod camouflage, using quantitative behavioral approaches alongside molecular techniques to characterize the identity, evolution and development of neuronal cell types.

Despite significant interest in this animal, a high-quality, annotated genome of its species is still lacking. To address this, we sequenced and assembled a chromosome-scale genome for *S. officinalis*. The final assembly spans 5.68 billion base pairs and comprises 47 repeat-rich chromosomes. Gene linkage analysis confirms the existence of 47 chromosomes, revealing clear homologies with related species such as *Euprymna scolopes* and *Doryteuthis pealeii*. Our work includes a comprehensive gene annotation and full-length transcript predictions that should be helpful for further evolutionary and single-cell expression studies. This genome provides a valuable resource for future research on the evolution, brain organization, information processing, development, and behavior in this important clade.

Introduction

Coleoid cephalopods (octopus, squid, cuttlefish) are a highly derived group of mollusks, characterized by the largest nervous systems among all invertebrates (ca. 500 million neurons in an adult octopus[1,2], ca. 200 million neurons in adult cuttlefish) and specializations with a great historical importance for neuroscience (e.g., “giant axons”[3] and “giant synapses”[4–6]). These animals exhibit very sophisticated behaviors such as dynamic camouflage[7–13], learning[14–16], social communication[17–19] and hunting[20–22] as well as two-stage sleep[23–25]. Because of these characteristics, cephalopods have been the focus of many fundamental studies by biologists, biophysicists and physiologists over the past century[26–35]. Thanks to advances in sequencing technologies, coleoid cephalopods are now also emerging as animal models in molecular neurobiology, evolution and genomics[36]. Recent studies in particular examined cephalopod biology from the perspectives of single-cell gene expression[37–40], genome topology and gene regulation[41].

Despite the technical progress, the genomes of cephalopods remain challenging to assemble because of their large sizes and high repeat fractions, creating a bottleneck for further molecular studies. While the genomes of *Octopodiformes* (Octopus, Eledone, Argonauta) are often comparable in size to that of humans (around 3 Gigabases (Gb)[42,43]) or possibly even smaller[44], the typical genomes of *Decapodiformes* (squids and cuttlefish) are often twice as large, reaching 6 Gb[45,46]. The biggest contributing factors to this genome expansion are transposable elements (TEs), with different TE classes differentiating squid and cuttlefish genomes from those of Octopodiformes[47]. Besides such differences in genome sizes, karyotypes in coleoid cephalopods are also unusual when compared to those of other invertebrates, including mollusks: for example, haploid chromosome numbers are around 30 in octopuses and around 46 in squids and cuttlefish[46,48], while they are between 8 and 19 in non-cephalopod mollusks[49–56]. Karyotype reconstruction and validation techniques in animals with such large genomes are also not as developed as they are for more familiar invertebrate and vertebrate species.

The common cuttlefish *Sepia officinalis* has been used as a model organism for studies in neural control and development[57,58], behavior[7,15], evolution[59], environmental studies[60,61] and biomechanics[62,63]. Found in the Mediterranean, the English Channel and the European Atlantic, it can produce large egg clutches containing hundreds of embryos, several times throughout its semelparous reproductive cycle[64,65]. More recently, this species has emerged as an important model to study the neural basis of cephalopod camouflage[66,67] building on

extensive behavioral studies[7–13] and neuronal cell type characterization, evolution and development[68–70].

Despite a widespread interest in this animal, including the recent sequencing of several cephalopod species as part of the Aquatic Symbiosis Genomics project[71], a high-quality, annotated genomic resource for this species is still lacking. We describe here the sequencing, assembly, and annotation of the *Sepia officinalis* genome. Our analysis provides evidence for the existence of 47 chromosomes, with clear homologies to the chromosomes of related species such as *Euprymna scolopes* and *Doryteuthis pealeii*. We predict full-length transcripts and provide functional gene annotation that should inform future evolutionary and transcriptomic studies. Taken together, this genome should be an important resource for scientists interested in genome evolution, brain organization, information processing, development and behavior.

Results

We sequenced the genome of a 6-month-old *Sepia officinalis* individual (probably male, see below), reared from eggs collected in the Portuguese Atlantic. The DNA was extracted from brain tissue and sequenced using long-read (PacBio HiFi) and chromatin conformation (Hi-C) methods (Figure 1A,B).

Genome size and heterozygosity

The haploid genome size of *S. officinalis* was estimated to be ~5.14 Gb based on k-mer estimation from the long-read data, with a high repeat content of 54 %[72,73]. The heterozygosity rate was estimated to be 1.03 %, which is higher than in octopus genomes, yet moderate among marine invertebrates[42,43,46].

The size of the scaffolded assembly was 5.68 Gb (Figure 1C), thus about 10% greater than our initial GenomeScope estimate. Indeed, the sizes of most published metazoan genome assemblies deviate by more than 10% from estimates, with proportionally greater deviations as assembly sizes increase[74].

Completeness of the genome was assessed using BUSCO[75] with *metazoa_odb10*. It was 95.2% [single copy: 93.5%, duplicated: 1.7%], with 3.2% fragmented and 1.6% missing BUSCOs. The BUSCO score with *mollusca_odb10* for the final assembly was 77.2%

102 completeness [single copy: 75.9%, duplicated: 1.3%] with 4.3% fragmented and 18.5%
103 missing BUSCOs.

104 Karyotype

105 The assembly was generated from PacBio HiFi reads and Hi-C reads with ca. 23-fold and
106 11-fold coverage, respectively. Scaffolding was performed using Hi-C reads, placing 95.8 %
107 of bases in 47 scaffolds. The Hi-C heatmap in Figure 1D shows the chromatin contacts in
108 clusters corresponding to these 47 scaffolds. It is consistent with the proposal that they each
109 represent a single chromosome.
110
111 To increase confidence in our assembled *Sepia officinalis* karyotype, we used several
112 scaffolding programs and manually curated the scaffolds using two independent
113 approaches. The first used HapHiC[76], a tool based on Hi-C data that utilizes allele
114 information from primary assembly programs, and scaffolds assemblies with the constraint of
115 an expected number of chromosomes. The resulting Hi-C contact maps with 46, 47, 48, 49
116 and 50 chromosomes (Supplementary Figure 1) show support for 47 chromosomes; an input
117 of 46 scaffolds resulted in one clear chromosome merger (blue arrowhead); higher input
118 numbers resulted in false chromosome splits (black arrowheads, 48, 49 and 50 scaffolds).
119
120 Second, we performed manual curation of the scaffolding result obtained with YAHS[77] using
121 JBAT[78]. These two approaches, conducted independently and both based on Hi-C signal,
122 converged on 47 chromosomal scaffolds.

123 Karyotype comparisons with other Decapods

124 Previous karyotyping studies in decapod cephalopods based on cytogenetic techniques
125 provide widely varying estimates of chromosome numbers, reflecting the difficulty of
126 resolving large chromosome numbers *in situ*. For example, 1n=46 chromosomes has been
127 reported for two species of cuttlefish (*Sepia esculenta* and *Sepia lycidas*) and three loliginid
128 squids[79]; 1n=34 chromosomes has been reported for *Sepia arabica*[80] and 1n=24
129 chromosomes in *Sepia pharaonis*[81]. In *Sepia officinalis*, a karyotype of 1n=52 has even been
130 described from testis samples[82]. More recently, several cephalopod genomes have been
131 scaffolded at chromosome-scale resolution, resolving karyotypes *in silico*. From those recent
132 studies, a haploid karyotype of 46 chromosomes seems to be common among
133 *Decapodiformes*[46] (Figure 2A).

Comparison with another chromosome-scale *Sepia officinalis* assembly

A chromosome-scale assembly for *Sepia officinalis* was released recently by the Wellcome Sanger Institute's Darwin Tree of Life project[83] (DToL, GCA_964300435.1). That genome was assembled from a male individual using PacBio Sequel II and Arima2 Hi-C data, with a final assembly size of 5.8 Gb. In that study, the haploid chromosome number was estimated to be 49. We scaffolded their assembly using our Dovetail Omni-C data, and the resulting contact map again supports 47 chromosomes (Supplementary Figure 2A), consistent with our results. We next aligned the two *S. officinalis* assemblies using minimap2[84] to assess the differences between them (Supplementary Figure 2B). The "Sanger" assembly appears to split three chromosomes of our assembly (chromosomes 1, 5 and 42) and to merge two (chromosomes 40 + 43). In conclusion, available evidence supports a haploid karyotype of 47 chromosomes in *Sepia officinalis*.

Comparisons with other chromosome-scale *Decapodiformes* genomes

To further investigate the possible reasons why our estimate of *Sepia officinalis's* chromosome numbers deviates from those in other studies, we compared our assembly with the chromosome-scale genomes of two other decapod cephalopods, *Euprymna scolopes*[41] (a *sepiolidae*) and *Doryteuthis pealeii*[46] (a *loliginidae*), both described as having 46 chromosomes. Using orthogroups to perform linkage analysis, we could detect a clear chromosome homology between *Doryteuthis* and *Sepia*, and to a lesser extent between *Euprymna* and *Sepia* (Figure 2B). Dotplots showing detailed pairwise synteny comparisons are shown in Supplementary Figure 3 (*Sepia* to *Doryteuthis*) and Supplementary Figure 4 (*Sepia* to *Euprymna*). The inferred species tree as part of this analysis places *Euprymna* as sister to *Sepia* and *Doryteuthis,* matching recent phylogenetic analyses[50,85]. However, this tree was constructed without the inclusion of outgroup taxa, and therefore lacks a reliable root.

This comparison revealed that chromosomes 40 and 43 in *Sepia* are merged into one in *Euprymna* and in *Dorytheutis* (Figure 2C), as they were in the DToL *Sepia officinalis* assembly (Supplementary Figure 2B). Our scaffolding approach showed no contact between chromosomes 40 and 43 in our *Sepia* Hi-C data, providing support for these chromosomes being separate in *Sepia officinalis*.

We also compared our assembly to a chromosome-scale *Sepia esculenta* assembly (1n=46, GCA_964036315.1), and recently annotated by genome liftover from *Sepia pharaonis*[86]. That assembly, constructed from a female individual, showed a low read coverage for a

169 putative sex chromosome in a ZZ/Z0 sex determination system[87]. Our syntenic comparison
170 indicated a strong homology between the putative Z chromosome of *Sepia esculenta* and
171 chromosome 46 of *Sepia officinalis* (Supplementary Figure 5A). Because we did not record
172 the sex of the *Sepia officinalis* animal used for genome sequencing and assembly, we tried
173 to infer the sex by replicating the analysis used to identify the putative Z chromosome in
174 *Sepia esculenta*[87]. For this, we aligned short-reads (Illumina) from the same *Sepia officinalis*
175 individual to the assembly and examined the normalized read coverage for each
176 chromosome (Supplementary Figure 5B). In contrast to the low coverage observed in the
177 female *Sepia esculenta* assembly (Supplementary Figure 5C), we observed no decrease in
178 read coverage for chromosome 46, suggesting that, if the alleged sex chromosome identity
179 is correct, then our material came from a male animal.

180 Genome repeat landscape

181 After creating a custom repeat library for *Sepia officinalis* using RepeatModeler[88], we
182 masked the genome using RepeatMasker[89], resulting in 71.17% masked bases. The
183 categories of repeats are shown in Figure 3A. Most repeats (39.65% of total bp) were not
184 characterized and presumably represent ancient repeats that diverged beyond recognition[90].
185 Retroelements constituted the largest characterized repeat category (17.32%) followed by
186 DNA transposons (5.92%); 5.83% were annotated as simple repeats. As observed in other
187 *Decapodiformes*, the *Sepia* genome contained almost no short interspersed nuclear
188 elements (SINEs), supporting the hypothesis that the SINE expansion observed in
189 octopuses[47] occurred independently in their lineage.

190 Gene modeling and annotation

191 The genome was further annotated using BRAKER[75,91–106] combining short- and long-read
192 RNA-seq data and publicly available protein data from multiple molluscan species
193 (*Doryteuthis pealeii*[46], *Euprymna scolopes*[107], *Octopus bimaculoides*[46], *Octopus vulgaris*[43],
194 *Nautilus pompilius*[108], and *Pecten maximus*[51]). A total of 18,663 gene models and 23,768
195 proteins were annotated.
196
197 The gene annotation was evaluated using BUSCO[75] v5.5.0 in protein mode, showing high
198 completeness of the annotation (metazoa_odb10: C:98.2%[S:77.3%,D:20.9%], F:1.0%,
199 M:0.8%, n:954 and mollusca_odb10: C:81.5%[S:59.6%,D:21.9%], F:0.9%, M:17.6%,
200 n:5295). We further checked the completeness and consistency of our gene models using
201 OMArk[109], and compared them to genome annotations for two other cuttlefish species, *Sepia*
202 *pharaonis* and *Sepia lycidas* (Figure 3B). The completeness is assessed by comparing the

203 annotated genes to conserved orthologs (present in 80% of extant species) in a given
204 taxonomic clade, here the superorder *Lophotrochozoa*. The *S. officinalis* annotation misses
205 181 out of 2373 genes, which is higher than *S. lycidas* (96 genes) but much lower than *S.*
206 *pharaonis* (458 genes).
207
208 In a consistency assessment, where the presence of known gene families from the lineage is
209 evaluated (Figure 3C), *S. officinalis* contains low proportions of taxonomically inconsistent or
210 fragmented proteins (ca. 13%) similar to *S. lycidas* (9%), giving confidence in the annotation.
211 In contrast, more than 50% of *S. pharaonis* proteins are labeled as inconsistent or
212 fragmented, which could indicate annotation errors[109].
213
214 Overall, the annotations contain different numbers of predicted proteins, likely caused by
215 differences in the annotation method and reference data used. *S. officinalis* contains the
216 least proteins (23,768) compared to *S. lycidas* (35,949) and *S. pharaonis* (53,515). The *S.*
217 *officinalis* annotation thus represents a conservative yet high-quality gene set. In the future,
218 this annotation could be enhanced by incorporating more long-read RNA sequencing data,
219 for example.
220
221 Lastly, we assigned orthology information to the *S. officinalis* proteome from InterPro[110] and
222 eggNOG-mapper[111] to aid the interpretability of the resource for future transcriptomic or
223 proteomic studies. Overall, 89% of proteins (21,204 out of 23,768) received an annotation
224 from InterPro from at least one of their databases. 59% of proteins (14,126 out of 23,768)
225 were annotated by eggNOG-mapper, reflecting the more stringent orthology filters and
226 prioritization of full-length matches implemented in the program[112]. Similar to previous
227 studies of other cephalopod genomes[42], we observed a high number of C2H2 zinc finger
228 transcription factors (1,538 proteins, InterPro annotation) and protocadherins (339 proteins,
229 InterPro), suggesting a conserved expansion of these gene families among cephalopods.
230 Further analyses should reveal more expanded gene families in *S. officinalis* that underlie
231 species-specific adaptations.

232 Discussion

233 This study presents a high-quality, chromosome-scale genome assembly and annotation for
234 the common cuttlefish *Sepia officinalis*, providing an additional important resource for
235 comparative genomics, neurobiology, and evolutionary studies within cephalopods and
236 mollusks. The assembly was derived from a combination of PacBio HiFi long reads, Dovetail

Omni-C chromatin conformation capture, and multiple rounds of scaffolding and manual curation, resulting in a genome size of 5.68 Gb and a haploid karyotype of 47 chromosomes. This resource represents a significant step forward for cephalopod genomics, especially within the *Decapodiformes*, where large and repetitive genomes have hindered previous efforts.

Chromosome Number and Karyotypic Variation

Our results strongly support a haploid chromosome number of 47 in *S. officinalis*, a conclusion reinforced by two independent scaffolding approaches (YAHS[77] and HapHiC[76]) and supported by Hi-C contact maps. This karyotype contrasts with the 46 chromosomes reported in other decapod cephalopods, such as *Euprymna scolopes* and *Doryteuthis pealeii*[46]. Syntenic comparisons revealed that chromosomes 40 and 43 in *S. officinalis* correspond to a single chromosome in these other species. The current Hi-C data for *Sepia officinalis* provides clear evidence that chromosomes 40 and 43 are distinct, with no interaction contact. Because these two chromosomes are merged also in *S. esculenta*, it is plausible that this difference results from a *S. officinalis*-specific fission. However, our results show how difficult it still is to assemble large genomes with high karyotype numbers. Therefore, validation and comparisons with other *Sepia* species' genomes will be important. This, in turn, will help identify chromosomal fusion-with-mixing events that are clade specific. Early branching order in *Decapodiformes* has been notoriously unstable[50,85,113–116]; thus, such rare and irreversible phylogenetic characters could be useful in further phylogenetic analysis of this clade[48,117].

We also compared our results to the recently published *S. officinalis* genome from the Darwin Tree of Life project (DToL)[83], which proposed 49 chromosomes. The discrepancy is attributable to one merger in our assembly and three apparent chromosome splits in the DToL assembly. While these differences could stem from technical choices such as different Hi-C methods (Arima v2 vs. Dovetail Omni-C) and sequencing depth (83-fold vs. 11-fold coverage), our assembly is strongly supported by Hi-C contact data, especially in regions where the DToL assembly splits chromosomes that appear contiguous in our data. Interestingly, the DToL assembly merges the chromosomes 40 and 43 - supporting a 46-chromosome model as ancestral state. However, this is not supported by re-scaffolding with the current Omni-C dataset, which again shows them as separate. This discrepancy might reflect technical differences, but it could also be hinting at population-level variability in chromosomal architecture; that is, some individuals may carry a fusion while others do not. Intraspecific chromosome number variation is rare but not unprecedented; for instance,

chromosomal polymorphism has been described in the butterfly *Leptidea sinapis* across different populations[118,119]. Notably, the two *S. officinalis* individuals used for sequencing originated from different regions - the Portuguese Atlantic (this study) and the French Mediterranean (DToL project), raising the possibility of geographic variation in chromosome structure. Future population-level analyses will be critical to determine whether *S. officinalis* exhibits karyotypic polymorphism.

Genome Size and Repeat Landscape

The size of the genome of *S. officinalis* is estimated at 5.68 Gb - comparable to other *Decapodiformes* and roughly double the size of typical *Octopodiformes* genomes. Repeat annotation revealed that over 71% of the genome is repetitive, dominated by unclassified elements and retrotransposons. The near absence of SINEs reinforces the idea that their expansion in octopuses was a lineage-specific event[47]. These results underscore the complexity and evolutionary dynamism of the cephalopod genome, shaped by waves of transposon activity that likely played a role in the evolution of novel traits[41,46].

Gene Annotation and Comparative Assessment

We annotated 18,663 gene models and 23,768 proteins using a combination of short- and long-read RNA-seq data and molluscan protein references. Compared with other annotated cuttlefish genomes (*S. lycidas*, *S. pharaonis*), our annotation is conservative in gene number but stands out in terms of completeness and taxonomic consistency. OMArk-based evaluations confirmed that our gene models have low levels of fragmentation and contamination, and high lineage-specific coherence. Striking differences across species in the number of predicted genes, duplications, and missing orthologs likely reflect variation in the annotation pipelines and reference data rather than true biological divergence. Still, our dataset provides a high-confidence foundation that can be refined with additional transcriptomic data from long-read techniques and diverse tissues.

As in other coleoid genomes, we observed notable expansions of gene families such as C2H2 zinc finger transcription factors and protocadherins, genes implicated in neural development and plasticity[42,45]. These conserved expansions across cephalopods point to genomic underpinnings of their cognitive complexity and behavioral sophistication.

Conclusions and Outlook

This study delivers a foundational genomic resource for *Sepia officinalis*, a model for studying neural control, behavior, and adaptive camouflage. The chromosome-scale assembly and annotation open the door to in-depth studies of gene regulation, neural circuit development, and genome evolution across coleoid cephalopods. Moreover, the identification of possible population-level karyotype variation highlights the importance of incorporating broader sampling strategies in future genomic studies.

As we move toward a more complete picture of cephalopod genome evolution, the integration of chromosomal synteny, regulatory architecture, and transcriptomic diversity across species will be especially important. The *S. officinalis* genome represents an important step on this path, enabling high-resolution comparative and functional analyses of one of the most enigmatic and evolutionarily successful invertebrate lineages.

Materials & Methods

Animal husbandry

All research and animal care procedures were carried out following the institutional guidelines that comply with national and international laws and policies (DIRECTIVE 2010/63/EU; German animal welfare act; FELASA guidelines). European cuttlefish *Sepia officinalis* were hatched from eggs collected in the Portuguese Atlantic and reared in a seawater system, at 20°C. The closed system contains 4,000l of artificial seawater (ASW; Instant Ocean) with a salinity of 33‰ and pH of 8–8.5. Water quality was tested daily and adjusted as required. Trace elements and amino acids were supplied weekly. Marine LED lights above each tank provided a 12/12-h light/dark cycle with gradual on- and off-sets at 07:00 and 19:00. The animals were fed live food (either *Hemimysis* spp. or small *Palaemonetes* spp.) *ad libitum* twice per day. The animals were housed together in 120-l glass tanks with a constant water through-flow resulting in five complete water exchanges per hour. Enrichment consisted of natural fine-grained sand substrate, seaweed (*Caulerpa prolifera*), rocks of different sizes and various natural and man-made three-dimensional objects.

Tissue preparation

Animals underwent terminal anesthesia to prevent animal suffering or distress, following the Guidelines for the Care and Welfare of Cephalopods in Research[120,121]. Animals were

331 transferred to a bucket containing ethanol 2% (v/v) in ASW. After 5 minutes, animals were
332 gently probed for simple avoidance reflexes, and the ethanol concentration in the ASW was
333 gradually increased to a maximum of 5%. Sufficient depth of anesthesia was reached when
334 the animal no longer reacted even to stronger stimuli (touching and pinching with tweezers),
335 and no reaction was observed when a hand was moved in the visual area and the cornea
336 was touched[122]. In this deep anesthesia, the animals were decapitated and the tissue was
337 rapidly transferred into ice-cold, calcium-free Ringer solution (460 mM NaCl, 10 mM KCl, 51
338 mM $MgCl_2$, 10 mM glucose, 2 mM Glutamine, 10 mM HEPES, pH 7.4) bubbled with oxygen.
339 Brain and body tissue was dissected under a stereoscope and flash-frozen in liquid nitrogen
340 before storage at -80ºC until further use.
341
342 Unless stated otherwise, sequencing libraries were prepared from the same individual (6-
343 month-old adult *Sepia officinalis*, F1 from eggs collected in Portugal).

344 Long-read Whole Genome Library Preparation and Sequencing

345 The long-read library was prepared and sequenced at the MPI for Plant Research in
346 Cologne, Germany. Genomic DNA was extracted from flash-frozen brain tissue with the
347 MagAttract HMW DNA kit (Qiagen, Cat. no. 67563) and the sequencing library was prepared
348 with the SMRTbell express template prep kit 2.0 (PacBio, Cat. no. 100-938-900). The library
349 was sequenced on 5 SMRT cells on the PacBio Sequel II with the Sequel II binding kit 2.2
350 (102-089-000), Sequel II sequencing kit 2.0 (101-820-200) and SMRT Cell 8M tray (101-
351 389-001).

352 Long-read RNA library preparation and sequencing

353 RNA was isolated from 5-10 mg of flash-frozen tissue (brain, mantle/epidermis,
354 arm/tentacle). First, tissue samples were homogenized in TRIzol using a homogenizer
355 (VDI12/S12N-5S, VWR, Germany). RNA was isolated and DNAseI treated according to the
356 Direct-zol RNA Mini prep kit from ZymoResearch (R2050). RNA was quantified by
357 spectrophotometry (Nanodrop, Thermo Scientific, USA) and its quality was assessed with a
358 RNA 6000 Nanochip on Bioanalyzer (Agilent Technologies, Germany).
359 The Iso-Seq libraries were prepared and sequenced at the Sequencing facility of the MPI for
360 Plant Research, using a method targeting the 5' cap and poly-A tail of mRNAs, described in
361 detail in[123]. Briefly, mRNA was pooled from the 8 tissue samples and cDNA was synthesized
362 using the TeloPrime Full-Length cDNA Amplification Kit V2 (Lexogen, Cat Nr: 013.08 or
363 013.24). The sequencing library was prepared with the SMRTbell express template prep kit
364 2.0 (PacBio, Cat. no. 100-938-900). The pooled library was sequenced on 1 SMRT cell on

365 the PacBio Sequel II system using the Sequel II binding kit 2.1 (101-843-000), Sequel II
366 sequencing kit 2.0 (101-820-200) and SMRT Cell 8M tray (101-389-001).
367 Further, a separate library was prepared from optic lobe cDNA and sequenced on a second
368 SMRT cell using the same reagents described above.

369 Omni-C Library Preparation and Sequencing

370 An Omni-C library was prepared and sequenced at the MPI for Plant Research in Cologne,
371 Germany. The library was prepared from brain tissue using the DovetailTM Omni-C™ Kit
372 (Dovetail Genomics, Cat. No. 21005) according to the manufacturer's protocol. Briefly,
373 chromatin was fixed in place in the nucleus. Fixed chromatin was digested with DNase I then
374 extracted. Chromatin ends were repaired and ligated to a biotinylated bridge adapter
375 followed by proximity ligation of adapter-containing ends. After proximity ligation, crosslinks
376 were reversed and the DNA was purified from proteins. Purified DNA was treated to remove
377 biotin that was not internal to ligated fragments. The sequencing library was generated using
378 Illumina-compatible adapters. Biotin-containing fragments were isolated using streptavidin
379 beads before PCR enrichment of the library. The library was sequenced on an Illumina
380 NextSeq 2000 platform to generate 400 million 2 x 150 bp read pairs.

381 Short-read DNA sequencing

382 High molecular weight genomic DNA was isolated from brain tissue (optic lobe) using NEB
383 Monarch gDNA Purification Kit (T3010S). First, 10 mg of flash-frozen tissue were submerged
384 in 100 µl of tissue lysis buffer, cut into small pieces and transferred into a 1.5 ml tube
385 containing an additional 100 µl of lysis buffer. Then, 3 µl of 20 U/µl Proteinase K was added
386 to the tissue sample and incubated for 2 h at 56°C in a thermal mixer with agitation until
387 tissue pieces were completely dissolved. After incubation, tissue lysate was purified from the
388 debris by centrifugation for 3 min at maximal speed (Eppendorf, Germany). Clean
389 supernatant was transferred to a new 1.5 ml tube and incubated with 3 µl RNase A for 5 min
390 at 56°C with agitation at full speed. After RNase A incubation tissue lysate was column
391 purified and eluted with 80 µl of elution buffer according to the manufacturer protocol. The
392 purity of gDNA was assessed using A260/280 and A260/230 absorbance ratios measured
393 by NanoDrop spectrophotometer (ThermoFisher Scientific). The integrity of the obtained
394 gDNA was checked using 0,75% agarose gel electrophoresis by loading 100 ng of gDNA
395 sample and using Hind III digested Lambda DNA (NEB#3012) as a marker.
396 DNA sequencing libraries were prepared from 500 ng of high MW gDNA using Illumina DNA
397 PCR-Free Tagmentation Library Prep Kit (20041794) and UD Indexes Set A (20026121).
398 Obtained dual-indexed single-stranded libraries were quantified using the Qubit single-

399 stranded DNA (ssDNA) assay kit (Q10212, ThermoFisher Scientific). 1000 pM of the final
400 library were run on P3 reagents and Illumina NextSeq2000 using Illumina DNA PCR-Free
401 Sequencing and Indexing primer (20041797) with 151 bp paired-end reads.

402 Short-read RNA library preparation and sequencing

403 For short-read RNA sequencing, tissue from another animal (8-month-old adult, F0 from
404 eggs collected in Normandie, France) was used. RNA was isolated from 5 mg of flash-frozen
405 tissues (brain, skin and retina). First, tissue samples were homogenized in TRIzol using a
406 homogenizer (VDI12/S12N-5S, VWR, Germany) following DNAseI treatment and column
407 purification according to the Direct-zol RNA Micro prep kit from ZymoResearch (R2062). The
408 RNA integrity and quantity were measured with the Qubit fluorometer (Invitrogen, Q33216)
409 and the 2100 Bioanalyzer (Agilent Technologies, Germany).
410 RNA-seq libraries were prepared from 300 ng of total RNA, using the Illumina TruSeq
411 stranded mRNA library prep kit (Cat:20020594) and IDT for Illumina xGen UDI-UMI Adapters
412 (Cat:10005903). Libraries were sequenced on an Illumina NextSeq500 (Mid output, 300 cyc)
413 and NextSeq2000 (P3, 300 cyc) with 145 bp paired-end reads.

414 Nuclear genome assembly

415 Before assembly, PacBio HiFi reads were subjected to additional trimming to remove
416 residual adapter sequences using NCBI's VecScreen tool. Genome size was estimated
417 using GenomeScope[72] from Illumina short reads and PacBio HiFi data. The primary
418 assembly was generated with hifiasm[124] using a combination of HiFi and Hi-C reads.
419 Scaffolding was performed iteratively with YAHS[77] on the phased haplotype 1. We adjusted
420 the run parameters for scaffolding resolutions (-r
421 1000,2000,5000,10000,20000,30000,50000,70000,100000,150000,200000,250000,300000,
422 350000,400000,500000,700000,1000000,2000000,5000000,10000000,15000000,20000000
423 ,30000000,40000000,50000000,60000000,70000000,80000000,100000000,110000000,120
424 000000,150000000,170000000,200000000,500000000), repetitions per resolution (-R3),
425 minimum read mapping quality (-q1) and telomeric sequence (--telo-motif "TTAGGG") from
426 the only experimentially determined telomere motif for cephalopods (*Amphioctopus*
427 *areolatus*[125], accessed via TeloBase[126]) to optimize the tool's performance for a large,
428 fragmented assembly. Finally, the assembly was manually curated using JBAT[78] to place
429 residual scaffolds into chromosome scaffolds. Different versions of the assembly were
430 evaluated based on HiC coverage, mRNA alignment and completeness based on BUSCO[75]
431 v5.5.0 (*metazoa_odb10* and *mollusca_odb10*).

Mitochondrial genome assembly

To assemble the mitochondrial genome, we aligned a published *S. officinalis* mitochondrial genome[127] (NC_007895.1) to the PacBio Hi-Fi and Omni-C reads using minimap2[84]. The hits were extracted using seqtk[128] subseq and assembled using hifiasm[124]. The resulting contigs contained multiple repeats of the circular mitochondrial genome, and were aligned back to NC_007895.1 to extract the final sequence.

Nuclear genome annotation

Repetitive elements in the genome were softmasked using RepeatMasker v4.1.7-p1[89] (with rmblast v2.14.1+) after creating a custom repeat library with RepeatModeler v.2.0.6[88].

Gene models were created using BRAKER3[75,91–106], run via the Docker container, on the softmasked genome using both RNA-seq and protein data. We used long-read Iso-Seq data and short-read Illumina RNA-seq data generated for this study (see above). For protein data, publicly available peptide annotations for *Doryteuthis pealeii*[46], *Euprymna scolopes*[107], *Octopus bimaculoides*[46], *Octopus vulgaris*[43], *Nautilus pompilius*[108], *Pecten maximus*[51] were used for training, as well as a previously generated proteome for *Sepia officinalis* from StringTie gene models (this study). RNA-seq data was input into BRAKER3 using the —bam option, protein files were specified with the–prot_seq option. The BUSCO completeness of the resulting gene set was maximized using TSEBRA within BRAKER on the BUSCO lineage *metazoa_odb10*.

For the initial protein set used as input for BRAKER, the short and long RNA reads were aligned to the genome using *minimap2*[84]. Transcript models were predicted with *StringTie* v3.0.0[129] using the *--conservative* and *--mix* options. The resulting GTF files were combined using the transcript merge mode, resulting in a set of non-redundant transcripts. Finally, TransDecoder[130] v5.7.0 was run with default parameters to translate coding regions in the transcripts.

The final gene annotations for *S. officinalis* were assessed for completeness using OMArk v.0.3.0[109] with the ancestral clade *Lophotrochozoa* and without including splice information, accessed via their webserver. Proteins were annotated with orthology information using InterProScan[110] v5.73-104 including lookup of annotations and GO terms (options -iprlookup -goterms). Further orthology information was added using the eggNOG-mapper v2.1.12[111] webserver with the eggNOG v5.0 database and default parameters.

466 ### Whole genome alignment and synteny analysis

467 For whole genome alignments, the assembly produced for *Sepia officinalis* in this study and
468 the published assembly from the Darwin Tree of Life project (GCA_964300435.1) were
469 aligned using *minimap2*[84] and visualized with a custom script in R v4.4.2[131].
470
471 For synteny analyses, peptide and gtf files were downloaded for *Doryteuthis pealeii* and
472 *Euprymna scolopes.* Annotation files for *Sepia esculenta* were recently generated by liftover
473 annotation from *Sepia pharaonis*[87] and downloaded from Zenodo[86]. Synteny analyses
474 between all chromosomes of the compared species were performed using the R package
475 GENESPACE v.1.2.3[132]. *S. officinalis* was used as the reference species for all synteny
476 maps.

477 ### Coverage analysis

478 Read coverage across chromosomes was analyzed as described recently[87]. Short reads
479 were aligned using STAR v2.7.11b[133] to our chromosome-scale assembly. For *Sepia*
480 *esculenta*, short reads (ERR12945500) and assembly (GCA_964036315.1) were
481 downloaded from NCBI. The sequencing depth was calculated using mosdepth[134] by a
482 window size of 500,000 bp and normalized to the median coverage of the first chromosome.

483 # Data availability

484 The genome assembly and raw sequencing reads can be found at the BioProject
485 PRJNA1091451 on NCBI. The code for the genome assembly and annotation is available at
486 https://gitlab.mpcdf.mpg.de/mpibr/laur/cuttlefishomics/soffgenome.
487 Genome annotation files are deposited at
488 https://public.brain.mpg.de/Laurent/sepoff/annotation/.

489 # Author contributions

490 O.S., and G.L. conceived of the study design. S.R., O.S. and G.L. wrote the first draft of the
491 manuscript. D.H. collected tissue for sequencing. E.C. extracted DNA and RNA from tissue
492 and performed Illumina sequencing. G.T. performed genome assembly. G.T. and S.R.
493 manually curated and annotated the genome. S.R., G.T., and O.S. performed genomic
494 analyses. S.R. created the figures. S.R., O.S. and G.L. coordinated and led the project. G.L.
495 acquired funding for this study.

All authors contributed to the review and editing of the manuscript.

Acknowledgments

We thank Bruno Huettel for PacBio and Omni-C sequencing. We thank Xitong Liang, Theodosia Woo and Mathieu Renard for help with tissue dissection. We thank Darrin Schultz, Dalila Destanović and Thea Rogers for helpful discussions and advice on manual curation and gene modeling.

This work was funded by the Max Planck Society (GL) and the European Research Council (GL; ERC grant CAMOUFLAGE, 101141501). O.S. was supported by the ERC's Horizon 2020: European Union Research and Innovation Programme, grant No. 945026.

All authors declare no conflict of interest. Views and opinions expressed are those of the authors only and do not necessarily reflect those of the European Union or the European Research Council Executive Agency. Neither the European Union nor the granting authority can be held responsible for them.

Figures

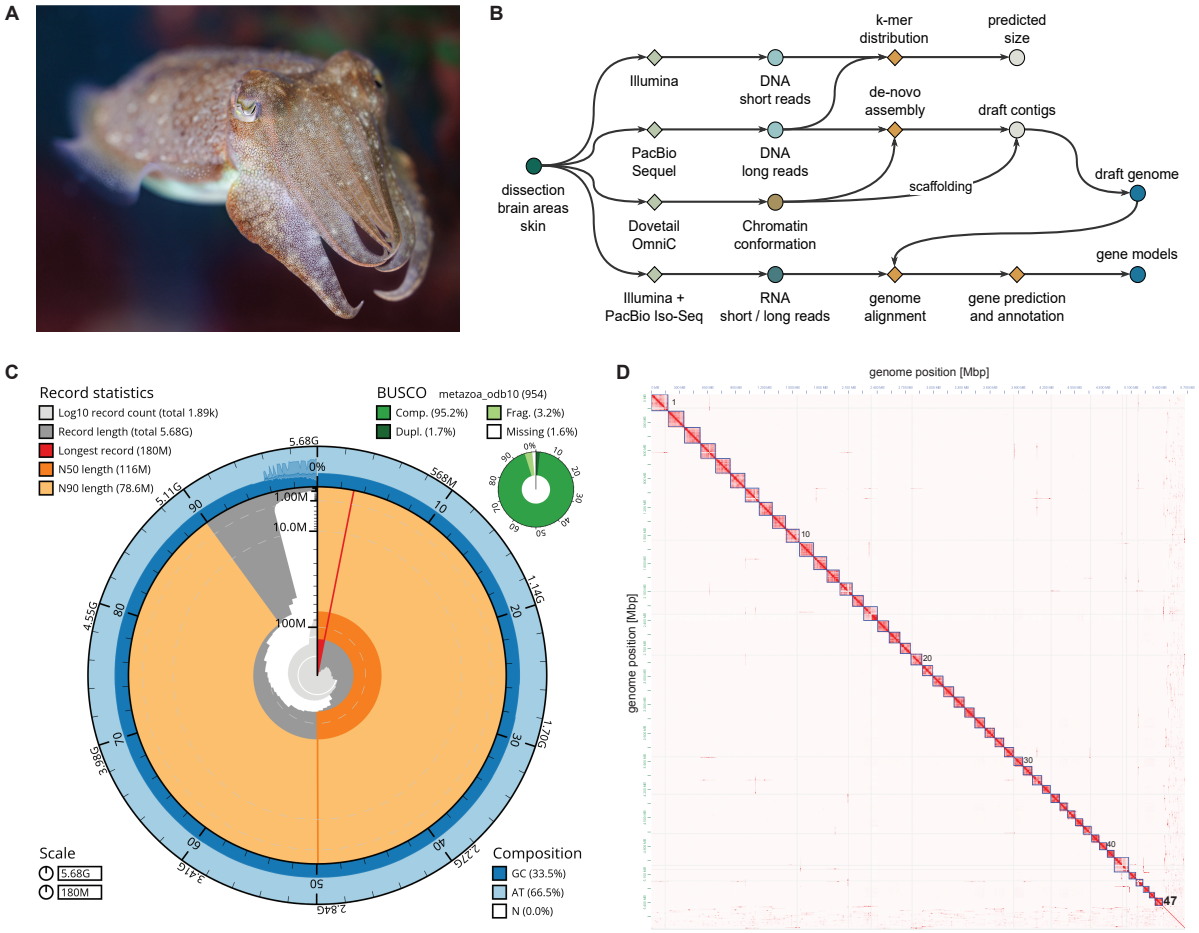

Figure 1: *Sepia officinalis* assembly statistics and quality control. A) Specimen of *S. officinalis* (credit: Stephan Junek, MPI Brain Research). **B)** Overview of the assembly workflow. Genome size was estimated using GenomeScope[72,73]. The primary assembly was generated from long DNA reads (PacBio Sequel II) and HiC reads (Dovetail OmniC) with hifiasm[124]. Assembly was scaffolded with YAHS[77]. **C)** Snail plot of chromosome-scale *S. officinalis* assembly generated using blobtools2[135] showing scaffold statistics, base composition and BUSCO[75] completeness against the metazoa_odb10 database. **D)** HiC heatmap showing 47 chromosome-scale scaffolds with very few sequences in unplaced scaffolds. Heatmap was generated using juicebox[78], 0-7039 observed counts (balanced) are shown.

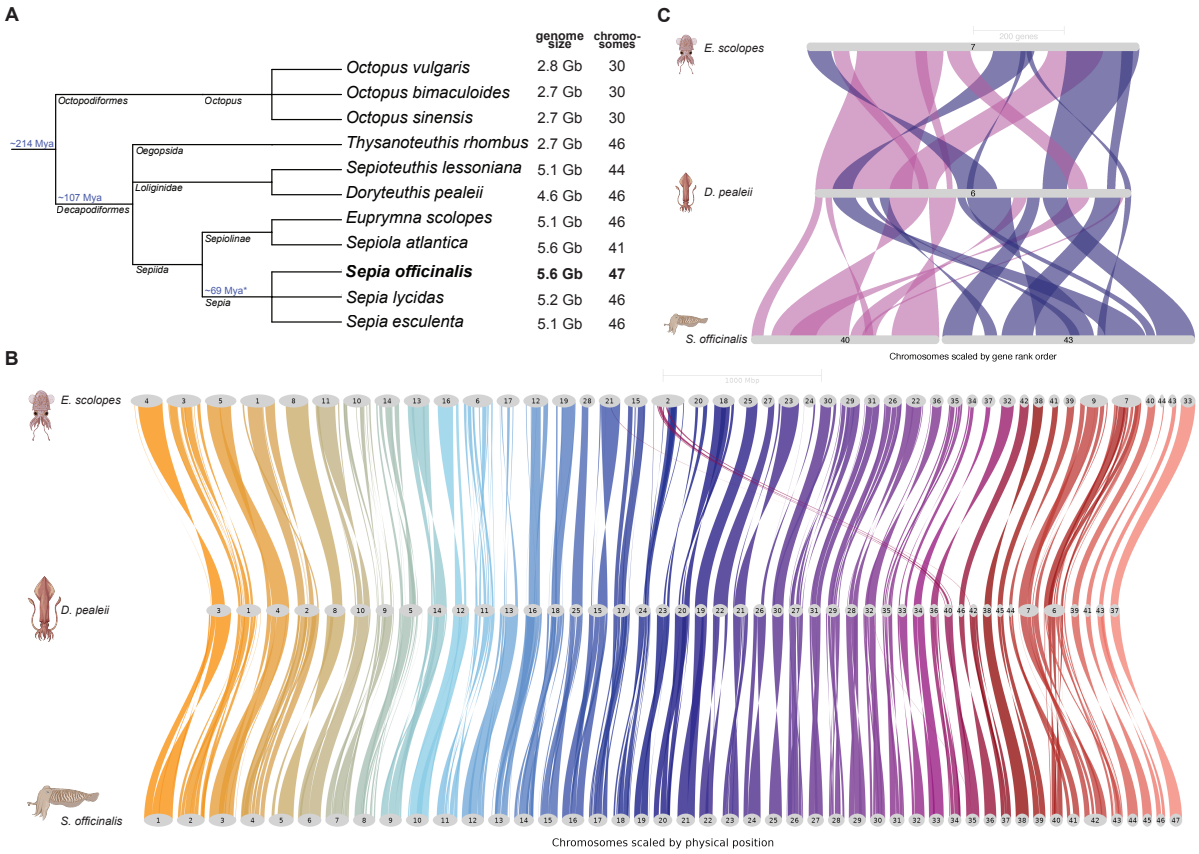

Figure 2: Syntenic comparison of three decapod species. A) Taxonomy of selected cephalopod species showing their genome size and (haploid) chromosome numbers. Taxonomy information downloaded from NCBI taxonomy browser, divergence times from[85,136]. **B)** Synteny relationship between chromosomes of *E. scolopes*[46] (top), *D. pealeii*[46] (middle) and *S. officinalis* (bottom). Riparian plot was generated using orthogroups located on chromosomes of the species. *Euprymna* chromosomes 45 and 46 are not shown because they contain too few orthogroups. **C)** Synteny plot of *Sepia* chromosomes 40 (magenta) and 43 (darkblue), that are joined in the other species and cause the different haploid chromosome number in *Sepia*. Species icons are from biorender.com.

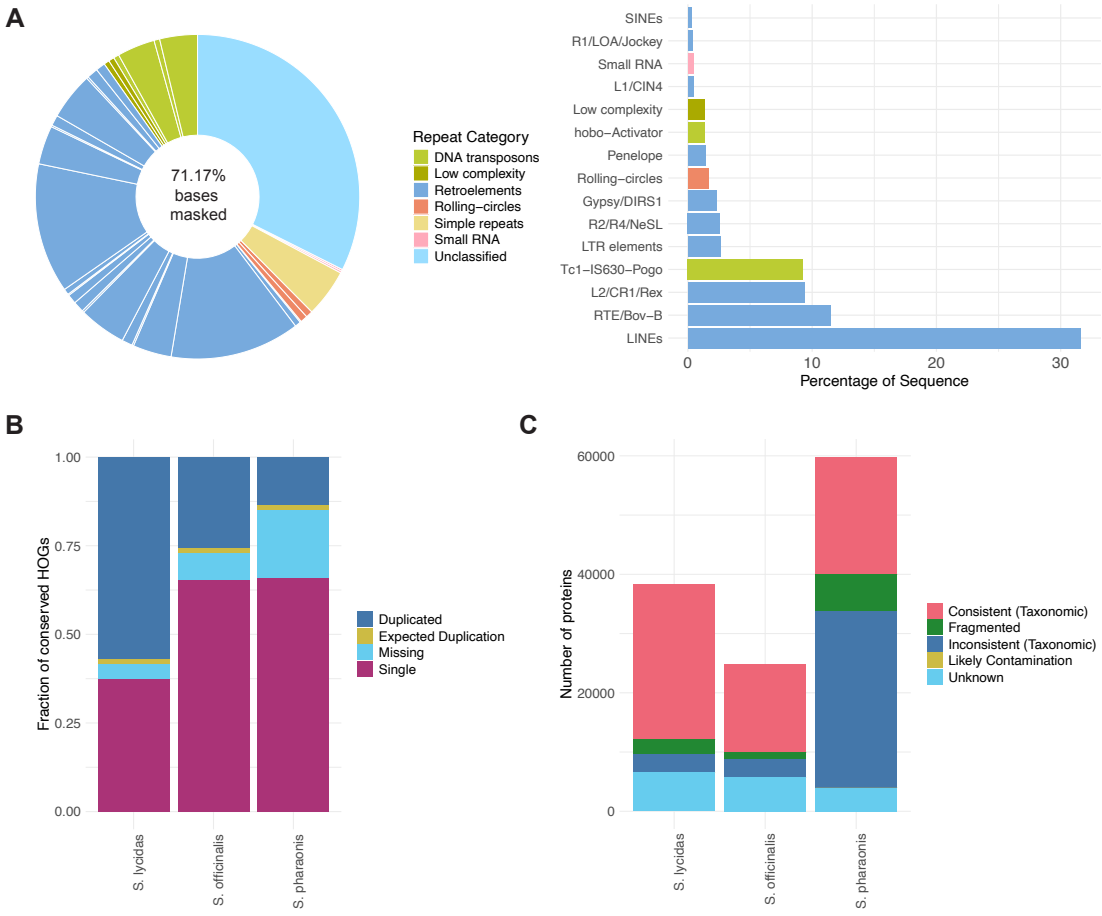

Figure 3: Genome annotation for *Sepia officinalis*. A) Annotation of repeat landscape of the *S. officinalis* genome, annotated using RepeatModeler[88]. Full repeat landscape is shown on the left, annotated repeats (excluding unclassified or simple repeats) are shown on the right. **B-C)** Quality control of gene annotation and comparison to two other cuttlefish species using OMArk[109]. Results shown for *Sepia lycidas* (GCA_963932145.1, Ensembl Genebuild), *Sepia officinalis* (BRAKER, this study) and *Sepia pharaonis*[137] (BRAKER). *Lophotrochozoa* was used as the ancestral clade. **B)** Completeness assessed by the presence of genes conserved in the clade, classified as *single* or multiple copies (*duplicated*), or *missing*. **C)** Consistency assessed by the proportion of proteins placed in the correct lineage (*consistent*); placement in incorrect lineages randomly (*inconsistent*) or to specific species (*contamination*), or no placement in known gene families (*unknown*).

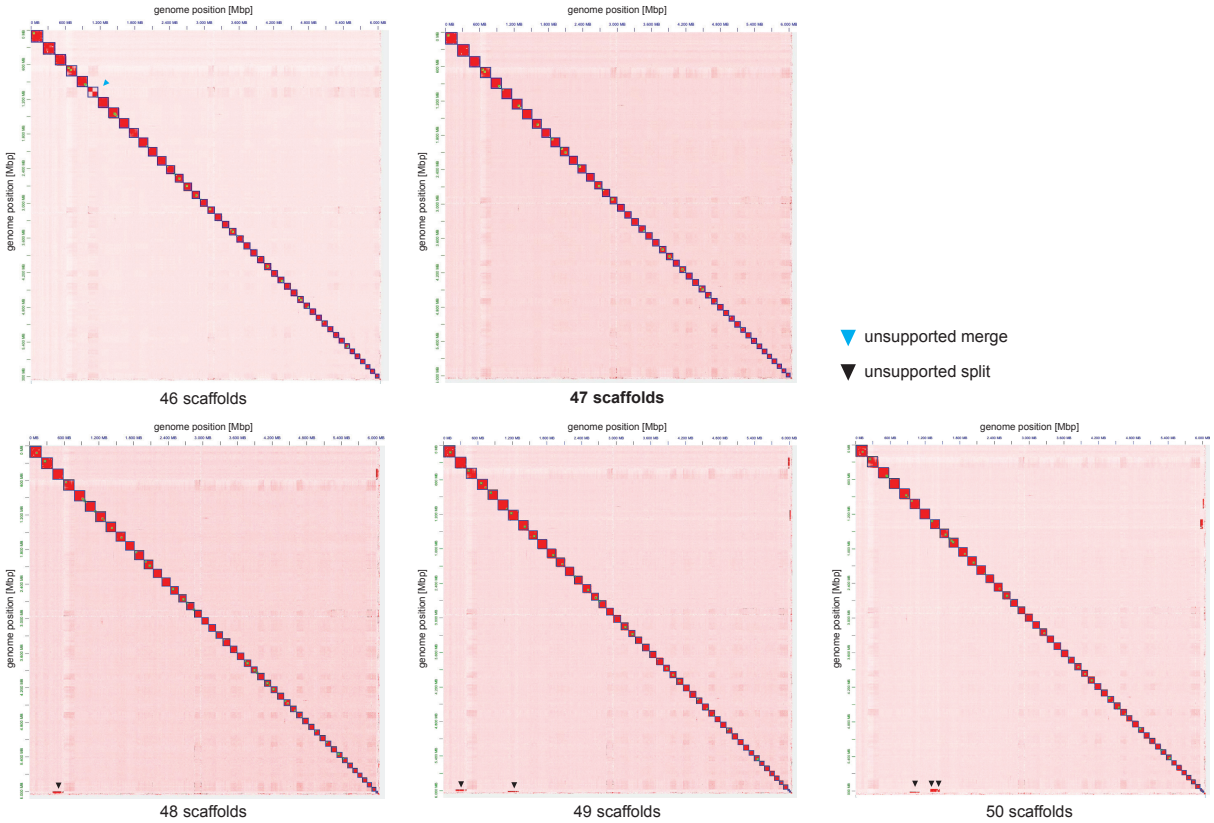

Supplementary Figure 1: HapHiC scaffolding for different numbers of expected chromosomes show 47 chromosomes as most supported. Hi-C contact maps from HapHiC[76] are shown for 46, 47, 48, 49 and 50 expected chromosome scaffolds. Assembled chromosomes are shown as blue boxes, HiC signal indicating a false (unsupported) merger is shown by cyan arrow, false splits are shown by black arrows.

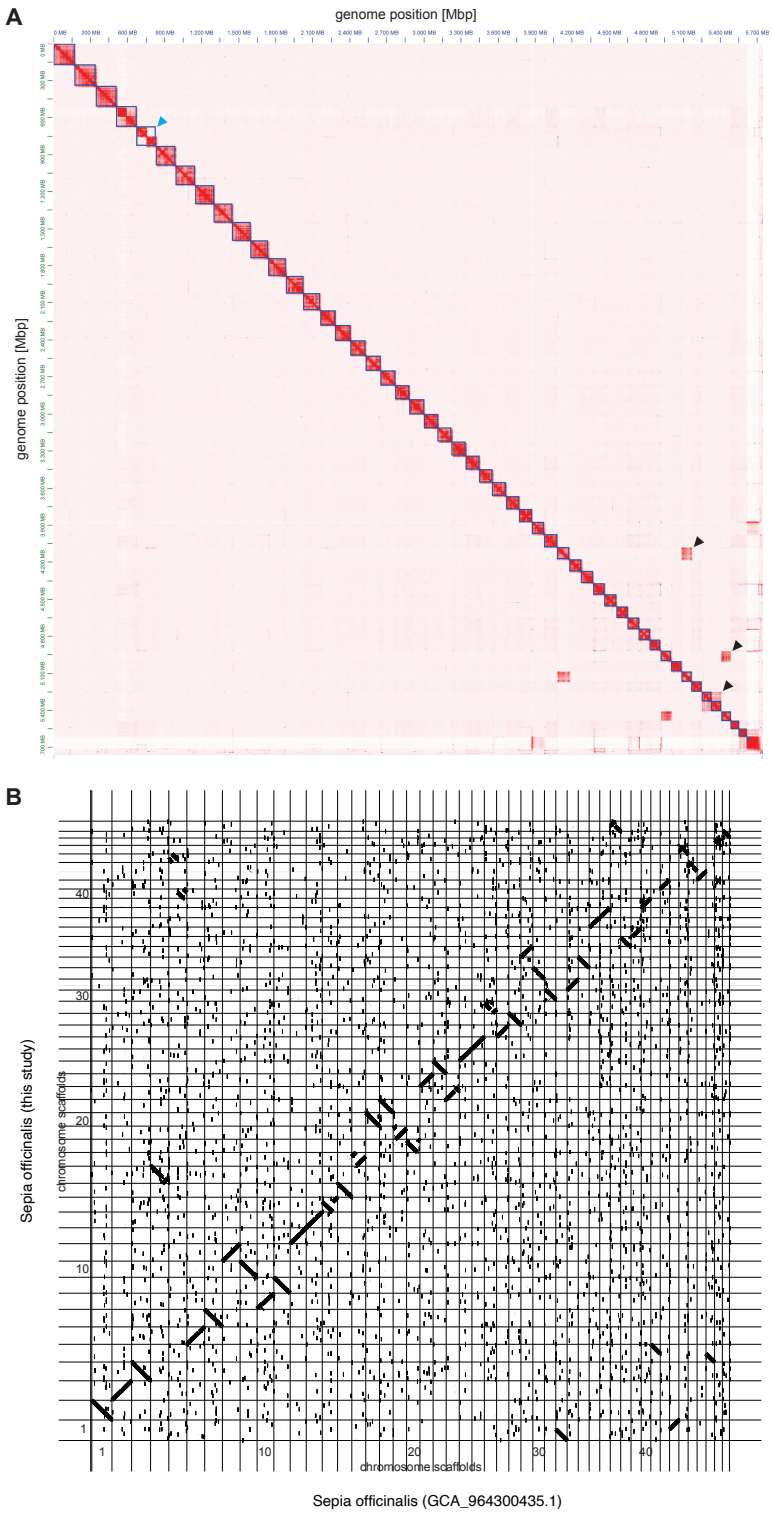

Supplementary Figure 2: Comparison of *Sepia officinalis* chromosome-scale assemblies. A) HiC heatmap of GCA_964300435.1 scaffolded against Omni-C data collected from a different individual (this study). Assembled chromosomes are shown as blue boxes, HiC signal indicating a false merge is shown by cyan arrow, false splits are shown by black arrows. **B)** Whole-genome alignment of both *S. officinalis* assemblies (this study: rows, GCA_964300435.1: columns).

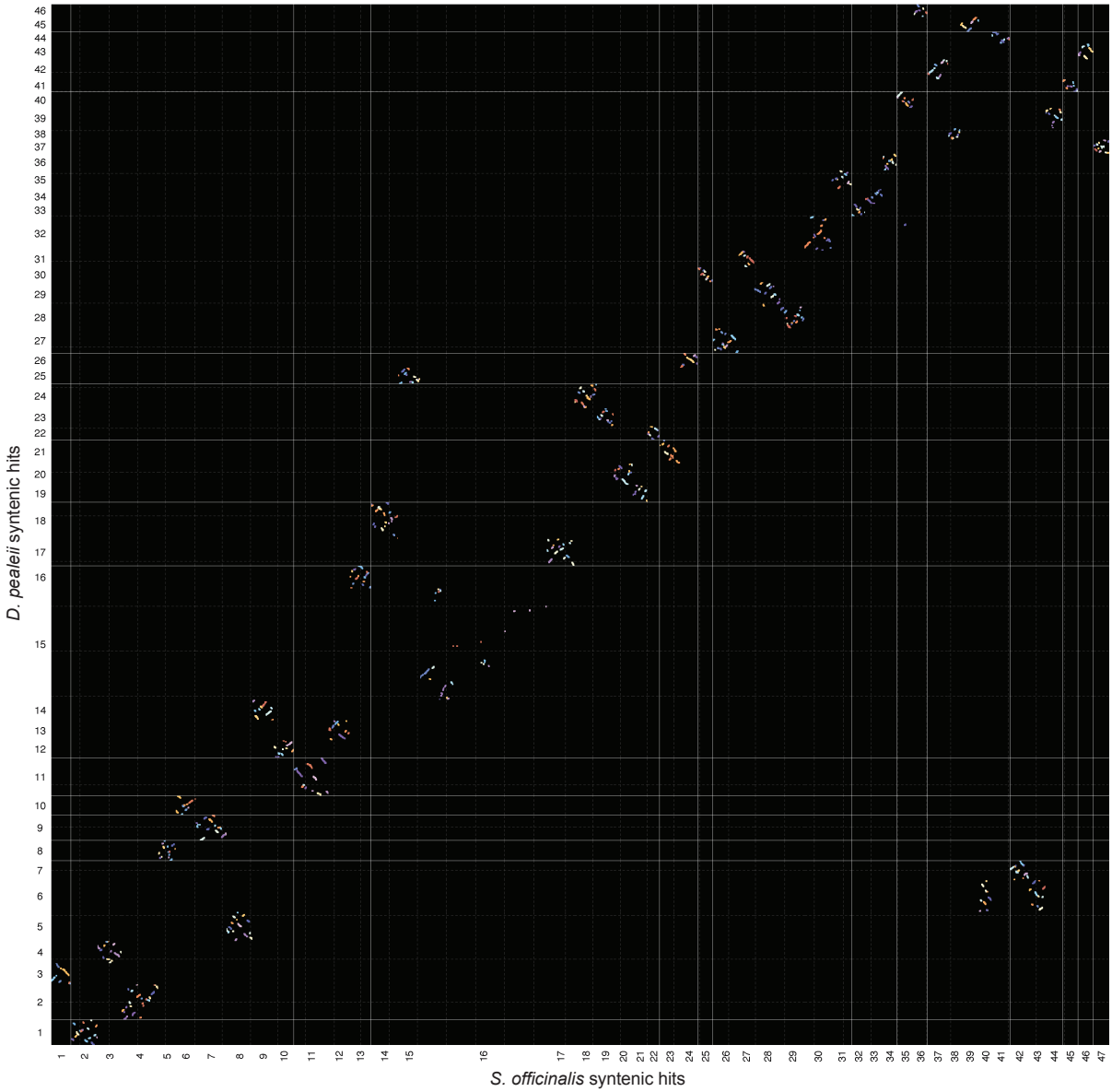

Supplementary Figure 3: Syntenic relationship between *S. officinalis* and *D. pealeii* chromosomes. Dot plot showing finer-resolution syntenic anchor hits (perfectly collinear blast hits within the same orthogroup). Genes are ordered along the chromosomes, gridlines are shown every 1000 genes.

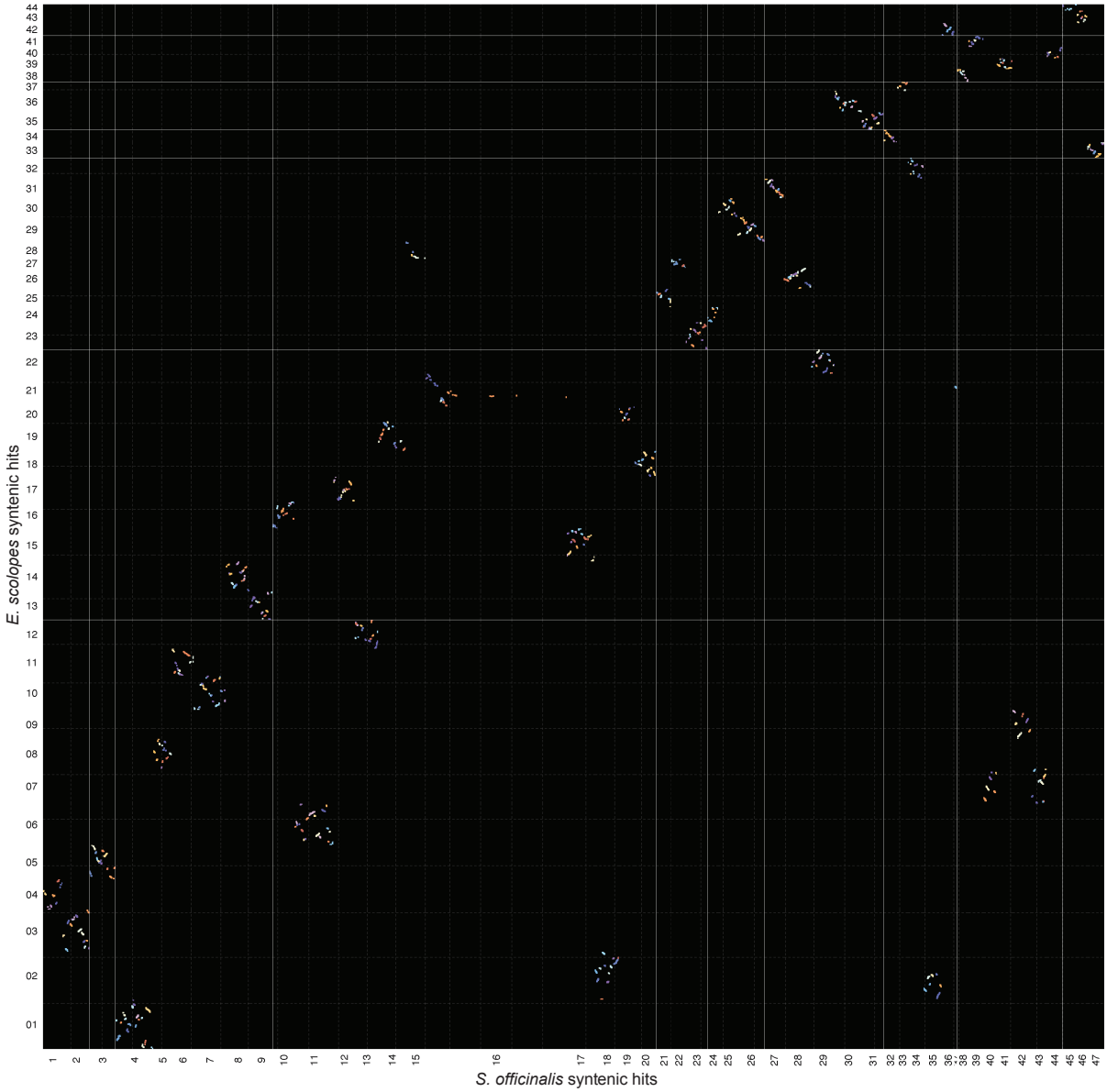

Supplementary Figure 4: Syntenic relationship between *S. officinalis* and *E. scolopes* chromosomes. Dot plot showing finer-resolution syntenic anchor hits (perfectly collinear blast hits within the same orthogroup). Genes are ordered along the chromosomes, gridlines are shown every 1000 genes. *E. scolopes* chromosomes 45 and 46 are not shown because they contain too few orthogroups.

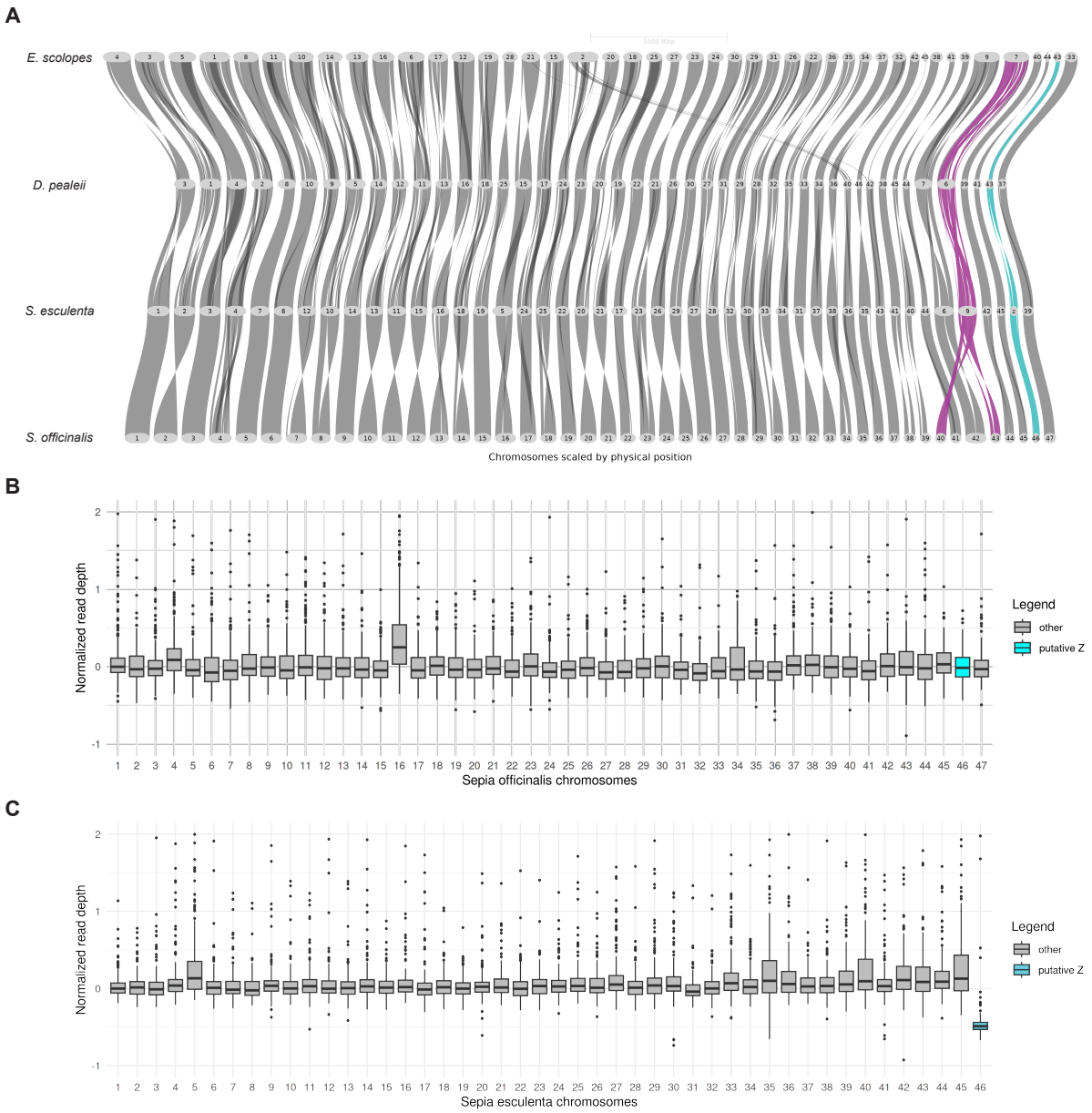

Supplementary Figure 5: Syntenic comparison of four decapod species hints at a cephalopod sex chromosome. A) Riparian plot showing synteny relationships of chromosomes from four decapod species, generated using orthogroups. *Euprymna* chromosomes 45 and 46 are not shown because they contain too few orthogroups. Chromosome split in *S. officinalis* compared to other species is shown in purple, putative sex chromosome as identified recently[87] is shown in cyan. **B)** Normalized coverage of sequencing data in *S. officinalis* chromosomes. **C)** Normalized coverage of short reads to female *S. esculenta* genome, reproduced from[87]. Decrease in read coverage for chromosome 46 visible, the putative Z sex chromosome. Read depth was calculated from Illumina gDNA reads in windows of 500,000 bp and normalized to the median coverage of chromosome 1. Box plots showing median divergence (box dividing line), interquartile range (box), and 1.5 times the interquartile range (whiskers). Putative Z chromosome is highlighted in cyan.

References

1. Giuditta, A., Libonati, M., Packard, A., and Prozzo, N. (1971). Nuclear counts in the brain lobes of octopus vulgaris as a function of body size. Brain Res. *25*, 55–62.

2. Young, J. (1963). The number and sizes of nerve cells in Octopus. In Proceedings of the Zoological Society of London (Wiley Online Library), pp. 229–254.

3. Hodgkin, A.L., Huxley, A.F., and Katz, B. (1952). Measurement of current-voltage relations in the membrane of the giant axon of Loligo. J. Physiol. *116*, 424–448. https://doi.org/10.1113/jphysiol.1952.sp004716.

4. Llinás, R., Steinberg, I.Z., and Walton, K. (1981). Presynaptic calcium currents in squid giant synapse. Biophys. J. *33*, 289–321. https://doi.org/10.1016/S0006-3495(81)84898-9.

5. Llinás, R., Steinberg, I.Z., and Walton, K. (1981). Relationship between presynaptic calcium current and postsynaptic potential in squid giant synapse. Biophys. J. *33*, 323–351. https://doi.org/10.1016/S0006-3495(81)84899-0.

6. Llinas, R.R. (1984). The Squid Giant Synapse. In Current Topics in Membranes and Transport The Squid Axon., A. Kleinzeller, ed. (Academic Press), pp. 519–546. https://doi.org/10.1016/S0070-2161(08)60483-9.

7. Hanlon, R.T., and Messenger, J.B. (2018). Cephalopod Behaviour 2nd ed. (Cambridge University Press) https://doi.org/10.1017/9780511843600.

8. Josef, N., Berenshtein, I., Rousseau, M., Scata, G., Fiorito, G., and Shashar, N. (2017). Size Matters: Observed and Modeled Camouflage Response of European Cuttlefish (Sepia officinalis) to Different Substrate Patch Sizes during Movement. Front. Physiol. *7*.

9. Osorio, D., Ménager, F., Tyler, C.W., and Darmaillacq, A.-S. (2022). Multi-level control of adaptive camouflage by European cuttlefish. Curr. Biol. *32*, 2556-2562.e2. https://doi.org/10.1016/j.cub.2022.04.030.

10. Marshall, N.J., and Messenger, J.B. (1996). Colour-blind camouflage. Nature *382*, 408–409. https://doi.org/10.1038/382408b0.

11. Zylinski, S., Osorio, D., and Shohet, A. j (2009). Perception of edges and visual texture in the camouflage of the common cuttlefish, Sepia officinalis. Philos. Trans. R. Soc. B

Biol. Sci. *364*, 439–448. https://doi.org/10.1098/rstb.2008.0264.

12. Zylinski, S., Darmaillacq, A.-S., and Shashar, N. (2012). Visual interpolation for contour completion by the European cuttlefish (Sepia officinalis) and its use in dynamic camouflage. Proc. R. Soc. B Biol. Sci. *279*, 2386–2390. https://doi.org/10.1098/rspb.2012.0026.

13. Zylinski, S., Osorio, D., and Shohet, A.J. (2009). Cuttlefish camouflage: context-dependent body pattern use during motion. Proc. R. Soc. B Biol. Sci. *276*, 3963–3969. https://doi.org/10.1098/rspb.2009.1083.

14. Jozet-Alves, C., Bertin, M., and Clayton, N.S. (2013). Evidence of episodic-like memory in cuttlefish. Curr. Biol. *23*, R1033–R1035. https://doi.org/10.1016/j.cub.2013.10.021.

15. Schnell, A.K., Boeckle, M., Rivera, M., Clayton, N.S., and Hanlon, R.T. (2021). Cuttlefish exert self-control in a delay of gratification task. Proc. R. Soc. B Biol. Sci. *288*, 20203161. https://doi.org/10.1098/rspb.2020.3161.

16. Boycott, B.B., and Young, J.Z. (1955). A memory system in Octopus vulgaris Lamarck. Proc. R. Soc. Lond. Ser. B - Biol. Sci. *143*, 449–480. https://doi.org/10.1098/rspb.1955.0024.

17. Mather, J.A. (2006). Behaviour Development: A Cephalopod Perspective. Int. J. Comp. Psychol. *19*. https://doi.org/10.46867/ijcp.2006.19.01.02.

18. Hall, K., and Hanlon, R. (2002). Principal features of the mating system of a large spawning aggregation of the giant Australian cuttlefish Sepia apama (Mollusca: Cephalopoda). Mar. Biol. *140*, 533–545.

19. Norman, M.D., Finn, J., and Tregenza, T. (1999). Female impersonation as an alternative reproductive strategy in giant cuttlefish. Proc. R. Soc. Lond. B Biol. Sci. *266*, 1347–1349. https://doi.org/10.1098/rspb.1999.0786.

20. Sampaio, E., Seco, M.C., Rosa, R., and Gingins, S. (2021). Octopuses punch fishes during collaborative interspecific hunting events. Ecology *102*, e03266. https://doi.org/10.1002/ecy.3266.

21. Sampaio, E., Sridhar, V.H., Francisco, F.A., Nagy, M., Sacchi, A., Strandburg-Peshkin, A., Nührenberg, P., Rosa, R., Couzin, I.D., and Gingins, S. (2024). Multidimensional social influence drives leadership and composition-dependent success in octopus–fish

hunting groups. Nat. Ecol. Evol. *8*, 2072–2084. https://doi.org/10.1038/s41559-024-02525-2.

22. Feord, R.C., Sumner, M.E., Pusdekar, S., Kalra, L., Gonzalez-Bellido, P.T., and Wardill, T.J. (2020). Cuttlefish use stereopsis to strike at prey. Sci. Adv. *6*, eaay6036. https://doi.org/10.1126/sciadv.aay6036.

23. Medeiros, S.L. de S., Paiva, M.M.M. de, Lopes, P.H., Blanco, W., Lima, F.D. de, Oliveira, J.B.C. de, Medeiros, I.G., Sequerra, E.B., de Souza, S., Leite, T.S., et al. (2021). Cyclic alternation of quiet and active sleep states in the octopus. iScience *24*, 102223. https://doi.org/10.1016/j.isci.2021.102223.

24. Iglesias, T.L., Boal, J.G., Frank, M.G., Zeil, J., and Hanlon, R.T. (2019). Cyclic nature of the REM sleep-like state in the cuttlefish Sepia officinalis. J. Exp. Biol. *222*, jeb174862. https://doi.org/10.1242/jeb.174862.

25. Pophale, A., Shimizu, K., Mano, T., Iglesias, T.L., Martin, K., Hiroi, M., Asada, K., Andaluz, P.G., Van Dinh, T.T., Meshulam, L., et al. (2023). Wake-like skin patterning and neural activity during octopus sleep. Nature *619*, 129–134. https://doi.org/10.1038/s41586-023-06203-4.

26. Young, J.Z. (1974). The central nervous system of Loligo I. The optic lobe. Philos. Trans. R. Soc. Lond. B Biol. Sci. *267*, 263–302.

27. Young, J.Z. (1962). The optic lobes of Octopus vulgaris. Philos. Trans. R. Soc. Lond. B. Biol. Sci. *245*, 19–58. https://doi.org/10.1098/rstb.1962.0005.

28. Young, J. (1960). The Visual System of Octopus:(1) Regularities in the Retina and Optic Lobes of Octopus in Relation to Form Discrimination. Nature *186*, 836–839.

29. Young, J.Z. (1991). Computation in the Learning System of Cephalopods. Biol. Bull. *180*, 200–208. https://doi.org/10.2307/1542389.

30. Young, J.Z. (1963). Light-and Dark-Adaptation in the Eyes of Some Cephalopods. Proc. Zool. Soc. Lond. *140*, 255–272. https://doi.org/10.1111/j.1469-7998.1963.tb01863.x.

31. Young, J.Z. (1962). The retina of cephalopods and its degeneration after optic nerve section. Philos. Trans. R. Soc. Lond. B. Biol. Sci. *245*, 1–18.

32. Nixon, M., and Young, J.Z. (2003). The brains and lives of cephalopods (Oxford University Press).

680 33. Case, N.M., Gray, E., and Young, J. (1972). Ultrastructure and synaptic relations in the
681 optic lobe of the brain of Eledone and Octopus. J. Ultrastruct. Res. *39*, 115–123.

682 34. Dilly, P., Gray, E.G., and Young, J.Z. (1963). Electron microscopy of optic nerves and
683 optic lobes of Octopus and Eledone. Proc. R. Soc. Lond. B Biol. Sci. *158*, 446–456.

684 35. Stephens, P., and Young, J.Z. (1969). The glio-vascular system of cephalopods. Philos.
685 Trans. R. Soc. Lond. B. Biol. Sci. *255*, 1–12.

686 36. Baden, T., Briseño, J., Coffing, G., Cohen-Bodénès, S., Courtney, A., Dickerson, D.,
687 Dölen, G., Fiorito, G., Gestal, C., Gustafson, T., et al. (2023). Cephalopod-omics:
688 Emerging Fields and Technologies in Cephalopod Biology. Integr. Comp. Biol. *63*, 1226–
689 1239. https://doi.org/10.1093/icb/icad087.

690 37. Styfhals, R., Zolotarov, G., Hulselmans, G., Spanier, K.I., Poovathingal, S., Elagoz, A.M.,
691 De Winter, S., Deryckere, A., Rajewsky, N., Ponte, G., et al. (2022). Cell type diversity in
692 a developing octopus brain. Nat. Commun. *13*, 7392. https://doi.org/10.1038/s41467-
693 022-35198-1.

694 38. Songco-Casey, J.O., Coffing, G.C., Piscopo, D.M., Pungor, J.R., Kern, A.D., Miller, A.C.,
695 and Niell, C.M. (2022). Cell types and molecular architecture of the Octopus
696 bimaculoides visual system. Curr. Biol. *0*. https://doi.org/10.1016/j.cub.2022.10.015.

697 39. Duruz, J., Sprecher, M., Kaldun, J.C., Al-Soudy, A.-S., Lischer, H.E., van Geest, G.,
698 Nicholson, P., Bruggmann, R., and Sprecher, S.G. (2023). Molecular characterization of
699 cell types in the squid Loligo vulgaris. eLife *12*, e80670.
700 https://doi.org/10.7554/eLife.80670.

701 40. Gavriouchkina, D., Tan, Y., Ziadi-Künzli, F., Hasegawa, Y., Piovani, L., Zhang, L.,
702 Sugimoto, C., Luscombe, N., Marlétaz, F., and Rokhsar, D.S. (2022). A single-cell atlas
703 of bobtail squid visual and nervous system highlights molecular principles of convergent
704 evolution. bioRxiv, 2022.05.26.490366. https://doi.org/10.1101/2022.05.26.490366.

705 41. Schmidbaur, H., Kawaguchi, A., Clarence, T., Fu, X., Hoang, O.P., Zimmermann, B.,
706 Ritschard, E.A., Weissenbacher, A., Foster, J.S., Nyholm, S.V., et al. (2022). Emergence
707 of novel cephalopod gene regulation and expression through large-scale genome
708 reorganization. Nat. Commun. *13*, 2172. https://doi.org/10.1038/s41467-022-29694-7.

709 42. Albertin, C.B., Simakov, O., Mitros, T., Wang, Z.Y., Pungor, J.R., Edsinger-Gonzales, E.,
710 Brenner, S., Ragsdale, C.W., and Rokhsar, D.S. (2015). The octopus genome and the

evolution of cephalopod neural and morphological novelties. Nature *524*, 220–224. https://doi.org/10.1038/nature14668.

43. Destanović, D., Schultz, D.T., Styfhals, R., Cruz, F., Gómez-Garrido, J., Gut, M., Gut, I., Fiorito, G., Simakov, O., Alioto, T.S., et al. (2023). A chromosome-level reference genome for the common octopus, Octopus vulgaris (Cuvier, 1797). G3 GenesGenomesGenetics, jkad220. https://doi.org/10.1093/g3journal/jkad220.

44. Yoshida, M., Hirota, K., Imoto, J., Okuno, M., Tanaka, H., Kajitani, R., Toyoda, A., Itoh, T., Ikeo, K., Sasaki, T., et al. (2022). Gene Recruitments and Dismissals in the Argonaut Genome Provide Insights into Pelagic Lifestyle Adaptation and Shell-like Eggcase Reacquisition. Genome Biol. Evol. *14*, evac140. https://doi.org/10.1093/gbe/evac140.

45. Belcaid, M., Casaburi, G., McAnulty, S.J., Schmidbaur, H., Suria, A.M., Moriano-Gutierrez, S., Pankey, M.S., Oakley, T.H., Kremer, N., Koch, E.J., et al. (2019). Symbiotic organs shaped by distinct modes of genome evolution in cephalopods. Proc. Natl. Acad. Sci. *116*, 3030–3035. https://doi.org/10.1073/pnas.1817322116.

46. Albertin, C.B., Medina-Ruiz, S., Mitros, T., Schmidbaur, H., Sanchez, G., Wang, Z.Y., Grimwood, J., Rosenthal, J.J.C., Ragsdale, C.W., Simakov, O., et al. (2022). Genome and transcriptome mechanisms driving cephalopod evolution. Nat. Commun. *13*. https://doi.org/10.1038/s41467-022-29748-w.

47. Marino, A., Kizenko, A., Wong, W.Y., Ghiselli, F., and Simakov, O. (2022). Repeat Age Decomposition Informs an Ancient Set of Repeats Associated With Coleoid Cephalopod Divergence. Front. Genet. *13*.

48. Simakov, O., Bredeson, J., Berkoff, K., Marletaz, F., Mitros, T., Schultz, D.T., O'Connell, B.L., Dear, P., Martinez, D.E., Steele, R.E., et al. (2022). Deeply conserved synteny and the evolution of metazoan chromosomes. Sci. Adv. *8*, eabi5884. https://doi.org/10.1126/sciadv.abi5884.

49. Zou, Y., Fu, J., Liang, Y., Luo, X., Shen, M., Huang, M., Chen, Y., You, W., and Ke, C. (2024). Chromosome-level genome assembly of the ivory shell Babylonia areolata. Sci. Data *11*, 1201. https://doi.org/10.1038/s41597-024-04001-9.

50. Chen, Z., Baeza, J.A., Chen, C., Gonzalez, M.T., González, V.L., Greve, C., Kocot, K.M., Arbizu, P.M., Moles, J., Schell, T., et al. (2025). A genome-based phylogeny for Mollusca is concordant with fossils and morphology. Science *387*, 1001–1007. https://doi.org/10.1126/science.ads0215.

743 51. Zeng, Q., Liu, J., Wang, C., Wang, H., Zhang, L., Hu, J., Bao, L., and Wang, S. (2021).
744 High-quality reannotation of the king scallop genome reveals no ‘gene-rich’ feature and
745 evolution of toxin resistance. Comput. Struct. Biotechnol. J. *19*, 4954–4960.
746 https://doi.org/10.1016/j.csbj.2021.08.038.

747 52. Sun, S., Han, X., Han, Z., and Liu, Q. (2024). Chromosomal-scale genome assembly
748 and annotation of the land slug (Meghimatium bilineatum). Sci. Data *11*, 35.
749 https://doi.org/10.1038/s41597-023-02893-7.

750 53. Männer, L., Schell, T., Spies, J., Galià-Camps, C., Baranski, D., Ben Hamadou, A.,
751 Gerheim, C., Neveling, K., Helfrich, E.J.N., and Greve, C. (2024). Chromosome-level
752 genome assembly of the sacoglossan sea slug Elysia timida (Risso, 1818). BMC
753 Genomics *25*, 941. https://doi.org/10.1186/s12864-024-10829-7.

754 54. Ma, B., Jin, W., Fu, H., Sun, B., Yang, S., Ma, X., Wen, H., Wu, X., Wang, H., and Cao,
755 X. (2023). A High-Quality Chromosome-Level Genome Assembly of a Snail
756 Cipangopaludina cathayensis (Gastropoda: Viviparidae). Genes *14*.
757 https://doi.org/10.3390/genes14071365.

758 55. Liu, Z., Huang, Y., Chen, H., Liu, C., Wang, M., Bian, C., Wang, L., and Song, L. (2023).
759 Chromosome-level genome assembly of the deep-sea snail Phymorhynchus
760 buccinoides provides insights into the adaptation to the cold seep habitat. BMC
761 Genomics *24*, 679. https://doi.org/10.1186/s12864-023-09760-0.

762 56. Peñaloza, C., Gutierrez, A.P., Eöry, L., Wang, S., Guo, X., Archibald, A.L., Bean, T.P.,
763 and Houston, R.D. (2021). A chromosome-level genome assembly for the Pacific oyster
764 Crassostrea gigas. GigaScience *10*, giab020.
765 https://doi.org/10.1093/gigascience/giab020.

766 57. Arias-Montecino, A., Sykes, A., Álvarez-Hernán, G., de Mera-Rodríguez, J.A., Calle-
767 Guisado, V., Martín-Partido, G., Rodríguez-León, J., and Francisco-Morcillo, J. (2024).
768 Histological and scanning electron microscope observations on the developing retina of
769 the cuttlefish (Sepia officinalis Linnaeus, 1758). Tissue Cell *88*, 102417.
770 https://doi.org/10.1016/j.tice.2024.102417.

771 58. O’Brien, C.E., Mezrai, N., Darmaillacq, A.-S., and Dickel, L. (2017). Behavioral
772 development in embryonic and early juvenile cuttlefish (Sepia officinalis). Dev.
773 Psychobiol. *59*, 145–160. https://doi.org/10.1002/dev.21476.

774 59. Bellingham, J., Morris, A.G., and Hunt, D.M. (1998). The Rhodopsin Gene of the

Cuttlefish Sepia Officinalis: Sequence and Spectral Tuning. J. Exp. Biol. *201*, 2299–2306. https://doi.org/10.1242/jeb.201.15.2299.

60. Chemello, G., Faraoni, V., Notarstefano, V., Maradonna, F., Carnevali, O., and Gioacchini, G. (2022). First Evidence of Microplastics in the Yolk and Embryos of Common Cuttlefish (Sepia officinalis) from the Central Adriatic Sea: Evaluation of Embryo and Hatchling Structural Integrity and Development. Anim. Open Access J. MDPI *13*. https://doi.org/10.3390/ani13010095.

61. Court, M., Macau, M., Ranucci, M., Marquês, T., Repolho, T., Lopes, V.M., Rosa, R., and Paula, J.R. (2024). Oxygen loss compromises growth and cognition of cuttlefish newborns. Proc. Biol. Sci. *291*, 20241291. https://doi.org/10.1098/rspb.2024.1291.

62. Gladman, N.W., and Askew, G.N. (2023). The hydrodynamics of jet propulsion swimming in hatchling and juvenile European common cuttlefish, Sepia officinalis. J. Exp. Biol. *226*. https://doi.org/10.1242/jeb.246225.

63. Yang, T., Jia, Z., Chen, H., Deng, Z., Liu, W., Chen, L., and Li, L. (2020). Mechanical design of the highly porous cuttlebone: A bioceramic hard buoyancy tank for cuttlefish. Proc. Natl. Acad. Sci. U. S. A. *117*, 23450–23459. https://doi.org/10.1073/pnas.2009531117.

64. Von Boletzky, S. (1987). Fecundity variation in relation to intermittent or chronic spawning in the cuttlefish, Sepia officinalis L. (Mollusca, Cephalopoda). Bull. Mar. Sci. *40*.

65. Laptikhovsky, V., Salman, A., Onsoy, B., and Katagan, T. (2003). Fecundity of the common cuttlefish, Sepia officinalis L. (Cephalopoda, Sepiidae): A new look at an old problem. Sci. Mar. *67*, 279–284.

66. Reiter, S., Hülsdunk, P., Woo, T., Lauterbach, M.A., Eberle, J.S., Akay, L.A., Longo, A., Meier-Credo, J., Kretschmer, F., Langer, J.D., et al. (2018). Elucidating the control and development of skin patterning in cuttlefish. Nature *562*, 361–366. https://doi.org/10.1038/s41586-018-0591-3.

67. Woo, T., Liang, X., Evans, D.A., Fernandez, O., Kretschmer, F., Reiter, S., and Laurent, G. (2023). The dynamics of pattern matching in camouflaging cuttlefish. Nature *619*, 122–128. https://doi.org/10.1038/s41586-023-06259-2.

68. Imarazene, B., Andouche, A., Bassaglia, Y., Lopez, P.-J., and Bonnaud-Ponticelli, L.

806 (2017). Eye Development in Sepia officinalis Embryo: What the Uncommon Gene
807 Expression Profiles Tell Us about Eye Evolution. Front. Physiol. *8*, 613.
808 https://doi.org/10.3389/fphys.2017.00613.

809 69. Cocci, P., Mosconi, G., and Palermo, F.A. (2023). Effect of polycyclic aromatic
810 hydrocarbons on homeobox gene expression during embryonic development of
811 cuttlefish, Sepia officinalis. Chemosphere *325*, 138315.
812 https://doi.org/10.1016/j.chemosphere.2023.138315.

813 70. Andouche, A., Bassaglia, Y., Baratte, S., and Bonnaud, L. (2013). Reflectin genes and
814 development of iridophore patterns in Sepia officinalis embryos (Mollusca,
815 Cephalopoda). Dev. Dyn. *242*, 560–571. https://doi.org/10.1002/dvdy.23938.

816 71. McKenna, V., Archibald, J., Beinart, R., Dawson, M., Hentschel, U., Keeling, P., Lopez,
817 J., Martin-Duran, J., Petersen, J., Sigwart, J., et al. (2024). The Aquatic Symbiosis
818 Genomics Project: probing the evolution of symbiosis across the Tree of Life [version 2;
819 peer review: 1 approved, 1 approved with reservations]. Wellcome Open Res. *6*.
820 https://doi.org/10.12688/wellcomeopenres.17222.2.

821 72. Ranallo-Benavidez, T.R., Jaron, K.S., and Schatz, M.C. (2020). GenomeScope 2.0 and
822 Smudgeplot for reference-free profiling of polyploid genomes. Nat. Commun. *11*, 1432.
823 https://doi.org/10.1038/s41467-020-14998-3.

824 73. Vurture, G.W., Sedlazeck, F.J., Nattestad, M., Underwood, C.J., Fang, H., Gurtowski, J.,
825 and Schatz, M.C. (2017). GenomeScope: fast reference-free genome profiling from short
826 reads. Bioinformatics *33*, 2202–2204. https://doi.org/10.1093/bioinformatics/btx153.

827 74. Hjelmen, C.E. (2024). Genome size and chromosome number are critical metrics for
828 accurate genome assembly assessment in Eukaryota. Genetics *227*, iyae099.
829 https://doi.org/10.1093/genetics/iyae099.

830 75. Simão, F.A., Waterhouse, R.M., Ioannidis, P., Kriventseva, E.V., and Zdobnov, E.M.
831 (2015). BUSCO: assessing genome assembly and annotation completeness with single-
832 copy orthologs. Bioinformatics *31*, 3210–3212.
833 https://doi.org/10.1093/bioinformatics/btv351.

834 76. Zeng, X., Yi, Z., Zhang, X., Du, Y., Li, Y., Zhou, Z., Chen, S., Zhao, H., Yang, S., Wang,
835 Y., et al. (2024). Chromosome-level scaffolding of haplotype-resolved assemblies using
836 Hi-C data without reference genomes. Nat. Plants *10*, 1184–1200.
837 https://doi.org/10.1038/s41477-024-01755-3.

838 77. Zhou, C., McCarthy, S.A., and Durbin, R. (2023). YaHS: yet another Hi-C scaffolding
839 tool. Bioinformatics *39*, btac808. https://doi.org/10.1093/bioinformatics/btac808.

840 78. Dudchenko, O., Shamim, M.S., Batra, S.S., Durand, N.C., Musial, N.T., Mostofa, R.,
841 Pham, M., Hilaire, B.G.S., Yao, W., Stamenova, E., et al. (2018). The Juicebox
842 Assembly Tools module facilitates de novo assembly of mammalian genomes with
843 chromosome-length scaffolds for under $1000. Preprint at bioRxiv,
844 https://doi.org/10.1101/254797 https://doi.org/10.1101/254797.

845 79. Gao, Y.M., and Natsukari, Y. (1990). Karyological studies on seven cephalopods. Venus
846 Jpn. J. Malacol. *49*, 126–145.

847 80. Jazayeri, A., Papan, F., Motamedi, H., and Mahmoudi, S. (2011). Karyological
848 investigation of Persian Gulf cuttle fish (sepia arabica) in the coasts of Khuzestan
849 province. Life Sci. J. *8*.

850 81. Ebrahimi Pour, M. (2009). The Study of Persian Gulf Cuttlefish (Sepia pharaonis)
851 Chromosome Via Incubation of Blood Cells. Appl. Biol. *22*, 1–8.
852 https://doi.org/10.22051/jab.2009.3307.

853 82. Vitturi, R., Rasotto, M.B., and Farinella-Ferruzza, N. (1982). The chromosomes of 16
854 molluscan species. Ital. J. Zool. *49*, 61–71.

855 83. The Darwin Tree of Life Project Consortium (2022). Sequence locally, think globally: The
856 Darwin Tree of Life Project. Proc. Natl. Acad. Sci. *119*, e2115642118.
857 https://doi.org/10.1073/pnas.2115642118.

858 84. Li, H. (2018). Minimap2: pairwise alignment for nucleotide sequences. Bioinformatics *34*,
859 3094–3100. https://doi.org/10.1093/bioinformatics/bty191.

860 85. López-Córdova, D.A., Avaria-Llautureo, J., Ulloa, P.M., Braid, H.E., Revell, L.J., Fuchs,
861 D., and Ibáñez, C.M. (2022). Mesozoic origin of coleoid cephalopods and their abrupt
862 shifts of diversification patterns. Mol. Phylogenet. Evol. *166*, 107331.
863 https://doi.org/10.1016/j.ympev.2021.107331.

864 86. Coffing, G., TITTES, S., Small, S., Songco-Casey, J.O., Pungor, J., Piscopo, D., Miller,
865 A., Niell, C., and Kern, A. (2024). Data for: Cephalopod Sex Determination and its
866 Ancient Evolutionary Origin. (Zenodo). https://doi.org/10.5281/zenodo.14010217
867 https://doi.org/10.5281/zenodo.14010217.

87. Coffing, G.C., Tittes, S., Small, S.T., Songco-Casey, J.O., Piscopo, D.M., Pungor, J.R., Miller, A.C., Niell, C.M., and Kern, A.D. (2025). Cephalopod sex determination and its ancient evolutionary origin. Curr. Biol. *35*, 931-939.e4. https://doi.org/10.1016/j.cub.2025.01.005.

88. Flynn, J.M., Hubley, R., Goubert, C., Rosen, J., Clark, A.G., Feschotte, C., and Smit, A.F. (2020). RepeatModeler2 for automated genomic discovery of transposable element families. Proc. Natl. Acad. Sci. *117*, 9451–9457. https://doi.org/10.1073/pnas.1921046117.

89. Smit, A., Hubley, R., and Green, P. RepeatMasker http://www.repeatmasker.org.

90. Feschotte, C. (2008). The contribution of transposable elements to the evolution of regulatory networks. Nat. Rev. Genet. *9*, 397–405. https://doi.org/10.1038/nrg2337.

91. Hoff, K.J., Lomsadze, A., Borodovsky, M., and Stanke, M. (2019). Whole-Genome Annotation with BRAKER. Methods Mol. Biol. Clifton NJ *1962*, 65–95. https://doi.org/10.1007/978-1-4939-9173-0_5.

92. Brůna, T., Hoff, K.J., Lomsadze, A., Stanke, M., and Borodovsky, M. (2021). BRAKER2: automatic eukaryotic genome annotation with GeneMark-EP+ and AUGUSTUS supported by a protein database. NAR Genomics Bioinforma. *3*, lqaa108. https://doi.org/10.1093/nargab/lqaa108.

93. Brůna, T., Gabriel, L., and Hoff, K.J. (2024). Navigating Eukaryotic Genome Annotation Pipelines: A Route Map to BRAKER, Galba, and TSEBRA. Preprint at arXiv, https://doi.org/10.48550/arXiv.2403.19416 https://doi.org/10.48550/arXiv.2403.19416.

94. Gabriel, L., Hoff, K.J., Brůna, T., Borodovsky, M., and Stanke, M. (2021). TSEBRA: transcript selector for BRAKER. BMC Bioinformatics *22*, 566. https://doi.org/10.1186/s12859-021-04482-0.

95. Hoff, K.J., Lange, S., Lomsadze, A., Borodovsky, M., and Stanke, M. (2016). BRAKER1: Unsupervised RNA-Seq-Based Genome Annotation with GeneMark-ET and AUGUSTUS. Bioinforma. Oxf. Engl. *32*, 767–769. https://doi.org/10.1093/bioinformatics/btv661.

96. Stanke, M., Schöffmann, O., Morgenstern, B., and Waack, S. (2006). Gene prediction in eukaryotes with a generalized hidden Markov model that uses hints from external sources. BMC Bioinformatics *7*, 62. https://doi.org/10.1186/1471-2105-7-62.

97. Stanke, M., Diekhans, M., Baertsch, R., and Haussler, D. (2008). Using native and syntenically mapped cDNA alignments to improve de novo gene finding. Bioinformatics *24*, 637–644. https://doi.org/10.1093/bioinformatics/btn013.

98. Li, H. (2023). Protein-to-genome alignment with miniprot. Bioinformatics *39*, btad014. https://doi.org/10.1093/bioinformatics/btad014.

99. Iwata, H., and Gotoh, O. (2012). Benchmarking spliced alignment programs including Spaln2, an extended version of Spaln that incorporates additional species-specific features. Nucleic Acids Res. *40*, e161. https://doi.org/10.1093/nar/gks708.

100. Gotoh, O. (2008). A space-efficient and accurate method for mapping and aligning cDNA sequences onto genomic sequence. Nucleic Acids Res. *36*, 2630–2638. https://doi.org/10.1093/nar/gkn105.

101. Buchfink, B., Xie, C., and Huson, D.H. (2015). Fast and sensitive protein alignment using DIAMOND. Nat. Methods *12*, 59–60. https://doi.org/10.1038/nmeth.3176.

102. Kovaka, S., Zimin, A.V., Pertea, G.M., Razaghi, R., Salzberg, S.L., and Pertea, M. (2019). Transcriptome assembly from long-read RNA-seq alignments with StringTie2. Genome Biol. *20*, 278. https://doi.org/10.1186/s13059-019-1910-1.

103. Brůna, T., Lomsadze, A., and Borodovsky, M. (2024). GeneMark-ETP significantly improves the accuracy of automatic annotation of large eukaryotic genomes. Genome Res. *34*, 757–768. https://doi.org/10.1101/gr.278373.123.

104. Huang, N., and Li, H. (2023). compleasm: a faster and more accurate reimplementation of BUSCO. Bioinformatics *39*, btad595. https://doi.org/10.1093/bioinformatics/btad595.

105. Pertea, G., and Pertea, M. (2020). GFF Utilities: GffRead and GffCompare. Preprint at F1000Research, https://doi.org/10.12688/f1000research.23297.2 https://doi.org/10.12688/f1000research.23297.2.

106. Gabriel, L., Brůna, T., Hoff, K.J., Ebel, M., Lomsadze, A., Borodovsky, M., and Stanke, M. (2024). BRAKER3: Fully automated genome annotation using RNA-seq and protein evidence with GeneMark-ETP, AUGUSTUS, and TSEBRA. Genome Res. *34*, 769–777. https://doi.org/10.1101/gr.278090.123.

107. Rogers, T.F., Yalçın, G., Briseno, J., Vijayan, N., Nyholm, S.V., and Simakov, O.

929 (2024). Gene modelling and annotation for the Hawaiian bobtail squid, Euprymna
930 scolopes. Sci. Data *11*, 40. https://doi.org/10.1038/s41597-023-02903-8.

931 108. Zhang, Y., Mao, F., Mu, H., Huang, M., Bao, Y., Wang, L., Wong, N.-K., Xiao, S., Dai,
932 H., Xiang, Z., et al. (2021). The genome of Nautilus pompilius illuminates eye evolution
933 and biomineralization. Nat. Ecol. Evol. *5*, 927–938. https://doi.org/10.1038/s41559-021-
934 01448-6.

935 109. Nevers, Y., Rossier, V., Train, C.M., Altenhoff, A., Dessimoz, C., and Glover, N.
936 (2022). Multifaceted quality assessment of gene repertoire annotation with OMArk.
937 bioRxiv, 2022.11.25.517970. https://doi.org/10.1101/2022.11.25.517970.

938 110. Blum, M., Andreeva, A., Florentino, L.C., Chuguransky, S.R., Grego, T., Hobbs, E.,
939 Pinto, B.L., Orr, A., Paysan-Lafosse, T., Ponamareva, I., et al. (2025). InterPro: the
940 protein sequence classification resource in 2025. Nucleic Acids Res. *53*, D444–D456.
941 https://doi.org/10.1093/nar/gkae1082.

942 111. Cantalapiedra, C.P., Hernández-Plaza, A., Letunic, I., Bork, P., and Huerta-Cepas, J.
943 (2021). eggNOG-mapper v2: Functional Annotation, Orthology Assignments, and
944 Domain Prediction at the Metagenomic Scale. Mol. Biol. Evol. *38*, 5825–5829.
945 https://doi.org/10.1093/molbev/msab293.

946 112. Huerta-Cepas, J., Forslund, K., Coelho, L.P., Szklarczyk, D., Jensen, L.J., von
947 Mering, C., and Bork, P. (2017). Fast Genome-Wide Functional Annotation through
948 Orthology Assignment by eggNOG-Mapper. Mol. Biol. Evol. *34*, 2115–2122.
949 https://doi.org/10.1093/molbev/msx148.

950 113. Tanner, A.R., Fuchs, D., Winkelmann, I.E., Gilbert, M.T.P., Pankey, M.S., Ribeiro,
951 Â.M., Kocot, K.M., Halanych, K.M., Oakley, T.H., da Fonseca, R.R., et al. (2017).
952 Molecular clocks indicate turnover and diversification of modern coleoid cephalopods
953 during the Mesozoic Marine Revolution. Proc. R. Soc. B Biol. Sci. *284*, 20162818.
954 https://doi.org/10.1098/rspb.2016.2818.

955 114. Anderson, F.E., and Lindgren, A.R. (2021). Phylogenomic analyses recover a clade
956 of large-bodied decapodiform cephalopods. Mol. Phylogenet. Evol. *156*, 107038.
957 https://doi.org/10.1016/j.ympev.2020.107038.

958 115. Lindgren, A.R., Pankey, M.S., Hochberg, F.G., and Oakley, T.H. (2012). A multi-gene
959 phylogeny of Cephalopoda supports convergent morphological evolution in association
960 with multiple habitat shifts in the marine environment. BMC Evol. Biol. *12*, 129.

https://doi.org/10.1186/1471-2148-12-129.

116. Sanchez, G., Setiamarga, D.H.E., Tuanapaya, S., Tongtherm, K., Winkelmann, I.E., Schmidbaur, H., Umino, T., Albertin, C., Allcock, L., Perales-Raya, C., et al. (2018). Genus-level phylogeny of cephalopods using molecular markers: current status and problematic areas. PeerJ *6*, e4331. https://doi.org/10.7717/peerj.4331.

117. Schultz, D.T., Haddock, S.H.D., Bredeson, J.V., Green, R.E., Simakov, O., and Rokhsar, D.S. (2023). Ancient gene linkages support ctenophores as sister to other animals. Nature *618*, 110–117. https://doi.org/10.1038/s41586-023-05936-6.

118. Lukhtanov, V.A., Dincă, V., Talavera, G., and Vila, R. (2011). Unprecedented within-species chromosome number cline in the Wood White butterfly Leptidea sinapis and its significance for karyotype evolution and speciation. BMC Evol. Biol. *11*, 109. https://doi.org/10.1186/1471-2148-11-109.

119. Lukhtanov, V.A., Dincă, V., Friberg, M., Šíchová, J., Olofsson, M., Vila, R., Marec, F., and Wiklund, C. (2018). Versatility of multivalent orientation, inverted meiosis, and rescued fitness in holocentric chromosomal hybrids. Proc. Natl. Acad. Sci. *115*, E9610–E9619. https://doi.org/10.1073/pnas.1802610115.

120. Ponte, G., Roumbedakis, K., COST Action FA1301, Galligioni, V., Dickel, L., Bellanger, C., Pereira, J., Vidal, E.A., Grigoriou, P., Alleva, E., et al. (2023). General and species-specific recommendations for minimal requirements for the use of cephalopods in scientific research. Lab. Anim. *57*, 26–39. https://doi.org/10.1177/00236772221111261.

121. Fiorito, G., Affuso, A., Basil, J., Cole, A., de Girolamo, P., D'Angelo, L., Dickel, L., Gestal, C., Grasso, F., Kuba, M., et al. (2015). Guidelines for the Care and Welfare of Cephalopods in Research –A consensus based on an initiative by CephRes, FELASA and the Boyd Group. Lab. Anim. *49*, 1–90. https://doi.org/10.1177/0023677215580006.

122. Andrews, P.L.R., Darmaillacq, A.-S., Dennison, N., Gleadall, I.G., Hawkins, P., Messenger, J.B., Osorio, D., Smith, V.J., and Smith, J.A. (2013). The identification and management of pain, suffering and distress in cephalopods, including anaesthesia, analgesia and humane killing. J. Exp. Mar. Biol. Ecol. *447*, 46–64. https://doi.org/10.1016/j.jembe.2013.02.010.

123. Cartolano, M., Huettel, B., Hartwig, B., Reinhardt, R., and Schneeberger, K. (2016). cDNA Library Enrichment of Full Length Transcripts for SMRT Long Read Sequencing.

PLOS ONE *11*, e0157779. https://doi.org/10.1371/journal.pone.0157779.

124. Cheng, H., Concepcion, G.T., Feng, X., Zhang, H., and Li, H. (2021). Haplotype-resolved de novo assembly using phased assembly graphs with hifiasm. Nat. Methods *18*, 170–175. https://doi.org/10.1038/s41592-020-01056-5.

125. Adachi, K., Ohnishi, K., Kuramochi, T., Yoshinaga, T., and Okumura, S.-I. (2014). Molecular cytogenetic study in Octopus (Amphioctopus) areolatus from Japan. Fish. Sci. *80*, 445–450. https://doi.org/10.1007/s12562-014-0703-4.

126. Lyčka, M., Bubeník, M., Závodník, M., Peska, V., Fajkus, P., Demko, M., Fajkus, J., and Fojtová, M. (2024). TeloBase: a community-curated database of telomere sequences across the tree of life. Nucleic Acids Res. *52*, D311–D321. https://doi.org/10.1093/nar/gkad672.

127. Akasaki, T., Nikaido, M., Tsuchiya, K., Segawa, S., Hasegawa, M., and Okada, N. (2006). Extensive mitochondrial gene arrangements in coleoid Cephalopoda and their phylogenetic implications. Mol. Phylogenet. Evol. *38*, 648–658. https://doi.org/10.1016/j.ympev.2005.10.018.

128. Li, H. (2013). Seqtk: a fast and lightweight tool for processing FASTA or FASTQ sequences.

129. Shumate, A., Wong, B., Pertea, G., and Pertea, M. (2022). Improved transcriptome assembly using a hybrid of long and short reads with StringTie. PLOS Comput. Biol. *18*, e1009730. https://doi.org/10.1371/journal.pcbi.1009730.

130. Haas, B.J. GitHub - TransDecoder/TransDecoder: TransDecoder source. https://github.com/TransDecoder/TransDecoder.

131. R Core Team (2024). R: A Language and Environment for Statistical Computing (R Foundation for Statistical Computing).

132. Lovell, J.T., Sreedasyam, A., Schranz, M.E., Wilson, M., Carlson, J.W., Harkess, A., Emms, D., Goodstein, D.M., and Schmutz, J. (2022). GENESPACE tracks regions of interest and gene copy number variation across multiple genomes. eLife *11*, e78526. https://doi.org/10.7554/eLife.78526.

133. Dobin, A., Davis, C.A., Schlesinger, F., Drenkow, J., Zaleski, C., Jha, S., Batut, P., Chaisson, M., and Gingeras, T.R. (2013). STAR: ultrafast universal RNA-seq aligner.

1023 Bioinforma. Oxf. Engl. *29*, 15–21. https://doi.org/10.1093/bioinformatics/bts635.

1024 134. Pedersen, B.S., and Quinlan, A.R. (2018). Mosdepth: quick coverage calculation for
1025 genomes and exomes. Bioinformatics *34*, 867–868.
1026 https://doi.org/10.1093/bioinformatics/btx699.

1027 135. Challis, R., Richards, E., Rajan, J., Cochrane, G., and Blaxter, M. (2020). BlobToolKit
1028 – Interactive Quality Assessment of Genome Assemblies. G3 GenesGenomesGenetics
1029 *10*, 1361–1374. https://doi.org/10.1534/g3.119.400908.

1030 136. Kröger, B., Vinther, J., and Fuchs, D. (2011). Cephalopod origin and evolution: A
1031 congruent picture emerging from fossils, development and molecules. BioEssays *33*,
1032 602–613. https://doi.org/10.1002/bies.201100001.

1033 137. Song, W., Li, R., Zhao, Y., Migaud, H., Wang, C., and Bekaert, M. (2021). Pharaoh
1034 Cuttlefish, Sepia pharaonis, Genome Reveals Unique Reflectin Camouflage Gene Set.
1035 Front. Mar. Sci. *8*.